© 2015. Published by The Company of Biologists Ltd | Journal of Cell Science (2015) 128, 2866-2880 doi:10.1242/jcs.167999

RESEARCH ARTICLE

The serotonin receptor 5-HT$_7$R regulates the morphology and migratory properties of dendritic cells

Katrin Holst[1], Daria Guseva[1], Susann Schindler[2], Michael Sixt[3], Armin Braun[2], Himpriya Chopra[4], Oliver Pabst[4,5] and Evgeni Ponimaskin[1,*]

ABSTRACT

Dendritic cells are potent antigen-presenting cells endowed with the unique ability to initiate adaptive immune responses upon inflammation. Inflammatory processes are often associated with an increased production of serotonin, which operates by activating specific receptors. However, the functional role of serotonin receptors in regulation of dendritic cell functions is poorly understood. Here, we demonstrate that expression of serotonin receptor 5-HT7 (5-HT$_7$R) as well as its downstream effector Cdc42 is upregulated in dendritic cells upon maturation. Although dendritic cell maturation was independent of 5-HT$_7$R, receptor stimulation affected dendritic cell morphology through Cdc42-mediated signaling. In addition, basal activity of 5-HT$_7$R was required for the proper expression of the chemokine receptor CCR7, which is a key factor that controls dendritic cell migration. Consistent with this, we observed that 5-HT$_7$R enhances chemotactic motility of dendritic cells *in vitro* by modulating their directionality and migration velocity. Accordingly, migration of dendritic cells in murine colon explants was abolished after pharmacological receptor inhibition. Our results indicate that there is a crucial role for 5-HT$_7$R–Cdc42-mediated signaling in the regulation of dendritic cell morphology and motility, suggesting that 5-HT$_7$R could be a new target for treatment of a variety of inflammatory and immune disorders.

KEY WORDS: 5-HT$_7$ receptor, Cdc42, Dendritic cell, Migration

INTRODUCTION

Serotonin (5-hydroxytryptamine, 5-HT) is one of the most extensively studied neurotransmitters in the central nervous system (CNS) regulating multiple physiological functions including the control of anger, aggression, body temperature, appetite, sleep, mood and pain (Mössner and Lesch, 1998). Serotonin operates by activating a family of specific 5-HT receptors, which comprise seven distinct classes based on their structural and functional characteristics. Serotonin receptors belong to the G-protein-coupled receptor family with exception of the 5-HT$_3$ receptor, which is an ion channel (Barnes and Sharp, 1999). Despite the major role of 5-HT in the CNS, ∼90% of 5-HT is produced in the gastro-intestinal tract (Racké et al., 1996), where it is involved in the regulation of multiple physiological processes such as stimulation of cytokine and chemokine production (Dürk et al., 2005; Idzko et al., 2004; Müller et al., 2009), cell proliferation (Pakala and Benedict, 1998; Pakala et al., 1997), migration (Kushnir-Sukhov et al., 2006; Müller et al., 2009; Tamura et al., 1997) and the regulation of the immune system (Ahern, 2011). Expression of 5-HT receptors has been identified on a broad range of immune cells, including T cells (O'Connell et al., 2006), macrophages (Mikulski et al., 2010) and dendritic cells (Idzko et al., 2004).

Dendritic cells are important innate immune cells, which are known as the most effective antigen-presenting cells (APCs). They play a key role in the induction of immune responses by capturing and transferring antigens to the cells of the adaptive immune system (Banchereau et al., 2000; Banchereau and Steinman, 1998; Figdor et al., 2004; Steinman and Witmer, 1978). In the steady state, immature dendritic cells continuously capture and take up self-antigens as well as injurious environmental proteins (Steinman et al., 2003). Following tissue damage, increased levels of inflammatory chemokines, cytokines, and foreign antigens (e.g. lipopolysaccharide, LPS) induce the maturation of dendritic cells (Ricart et al., 2011). During this process, dendritic cells lose the ability to further uptake and process antigens, while gaining the capacity to activate T cells (Banchereau et al., 2000; Langenkamp et al., 2000; Roses et al., 2008). For that, mature dendritic cells have to migrate to the secondary lymphoid organs, where they directly interact with naïve T cells to initiate immune responses (Banchereau and Steinman, 1998; Harada et al., 2012; Müller et al., 2009; Randolph et al., 2005; Steinman, 1991). In addition, maturating dendritic cells undergo fundamental morphological changes by cytoskeleton reorganizations leading to the development of cellular extensions (Hubo et al., 2013; Verdijk et al., 2004). Maturation is an essential factor for dendritic cell functions, because this process includes the upregulated surface expression of the crucial chemokine receptor CCR7, which drastically enhances migratory capacity of cells (Ricart et al., 2011; Sallusto et al., 1999; Yanagihara et al., 1998). Beside the chemokine receptor CCR7, 5-HT receptors expression profiles are also altered during maturation of dendritic cells. It has been demonstrated that immature dendritic cells highly express 5-HT$_{1B}$R, 5-HT$_{1E}$R and 5-HT$_{2B}$R, whereas mature dendritic cells show expression of 5-HT$_4$R and 5-HT$_7$R (Idzko et al., 2004). The 5-HT$_7$R is one of the most recently identified members of the 5-HT receptor family. Its activation induces cAMP elevation through the stimulatory G$_s$ protein (Albayrak et al., 2013; Hedlund, 2009) and upregulates the release of pro-inflammatory cytokines and co-stimulatory molecules for T cell activation in mature dendritic cells (Dienz and Rincon, 2009; Müller et al., 2009). It has also been shown that in neurons 5-HT$_7$R is involved in regulation of neuronal morphology through the G$_{12}$-protein-mediated activation of the small GTPase Cdc42 (Kvachnina et al., 2005; Ponimaskin et al., 2007).

Although Cdc42 involvement in dendritic cell morphology and motility has been intensively studied during the last decade, the

[1]Cellular Neurophysiology, Hannover Medical School, Hannover 30625, Germany. [2]Department of Airway Immunology, Fraunhofer Institute for Toxicology and Experimental Medicine, Hannover 30625, Germany. [3]Institute of Science and Technology Austria, Klosterneuburg 3400, Austria. [4]Institute of Immunology, Hannover Medical School, Hannover 30625, Germany. [5]Institute of Molecular Medicine, RWTH Aachen University, Aachen 52074, Germany.

*Author for correspondence (Ponimaskin.Evgeni@mh-hannover.de)

Received 23 December 2014; Accepted 15 June 2015

Journal of Cell Science

Journal of Cell Science (2015) 128, 2866-2880 doi:10.1242/jcs.167999

regulatory upstream mechanisms controlling Cdc42 functions have not been elucidated so far. In the present study, we demonstrate that expression of the 5-HT$_7$R and Cdc42 is significantly increased in dendritic cells upon maturation. Although maturation of dendritic cells was not influenced by 5-HT$_7$R, stimulation of the 5-HT$_7$R–Cdc42 signaling pathway influenced formation and elongation of cellular processes in mature bone-marrow-derived dendritic cells (BMDCs). Moreover, our data demonstrate that, in dendritic cells, 5-HT$_7$R-mediated signaling is involved in regulation of the expression level of the chemokine receptor CCR7. In addition, our data show that 5-HT$_7$R plays an important role in the regulation of chemotactic motility of BMDCs under *in vitro* conditions by modulating directionality and migration velocity. Accordingly, the dendritic cell migration in colon preparations from mice was significantly decreased after pharmacological receptor inhibition. Taken together, our results suggest that 5-HT$_7$R–Cdc42-mediated signaling regulates dendritic cell morphology and migration, and thus might represent an attractive target for the treatment of a variety of inflammatory and immune diseases.

RESULTS

Expression of 5-HT$_7$R is upregulated upon maturation of BMDCs

It has been suggested that different effects of serotonin on immune cells might be mediated by the variable expression of the corresponding 5-HT receptors (Idzko et al., 2004). Therefore, we analyzed whether the expression of 5-HT$_7$R changes upon dendritic cell maturation. For that, we determined receptor expression profiles in immature and mature BMDCs using quantitative real-time PCR (qRT-PCR). Maturation of BMDCs was induced by LPS treatment for 48 h. As shown in Fig. 1A, BMDC maturation caused a significant upregulation of the 5-HT$_7$R mRNA level (9.5-fold) as compared to immature BMDCs (Fig. 1A). Given that the level of mRNA transcripts do not necessarily correlate with the protein expression level, we analyzed protein expression of 5-HT$_7$R in mature and immature BMDCs by western blot analysis. In line with transcript levels, protein expression of 5-HT$_7$R in membrane fractions significantly increased upon BMDC maturation (Fig. 1B). Immunocytochemical analysis further confirmed a higher expression of 5-HT$_7$R in mature BMDCs (Fig. 1C). Taken together, these results demonstrate upregulation of 5-HT$_7$R during maturation of BMDCs.

5-HT$_7$R-mediated signaling does not affect differentiation and maturation of BMDCs

To investigate the functional impact of 5-HT$_7$R on dendritic cell development, we compared the maturation profile of BMDCs isolated from wild-type (WT) and 5-HT$_7$R-deficient mice. Flow cytometry analysis revealed a similar expression profile of several well-established dendritic cell surface markers, such as major histocompatibility complex class II (MHC II) molecules, CD11c (also known as ITGAX) and CD86 in LPS-stimulated mature 5-HT$_7$R-deficient and WT BMDCs (Fig. 2A,B). Similar results were obtained in immature BMDCs (data not shown). In addition, the number and ratio of mature and immature BMDCs in WT and 5-HT$_7$R-deficient BMDC cell cultures was quite similar

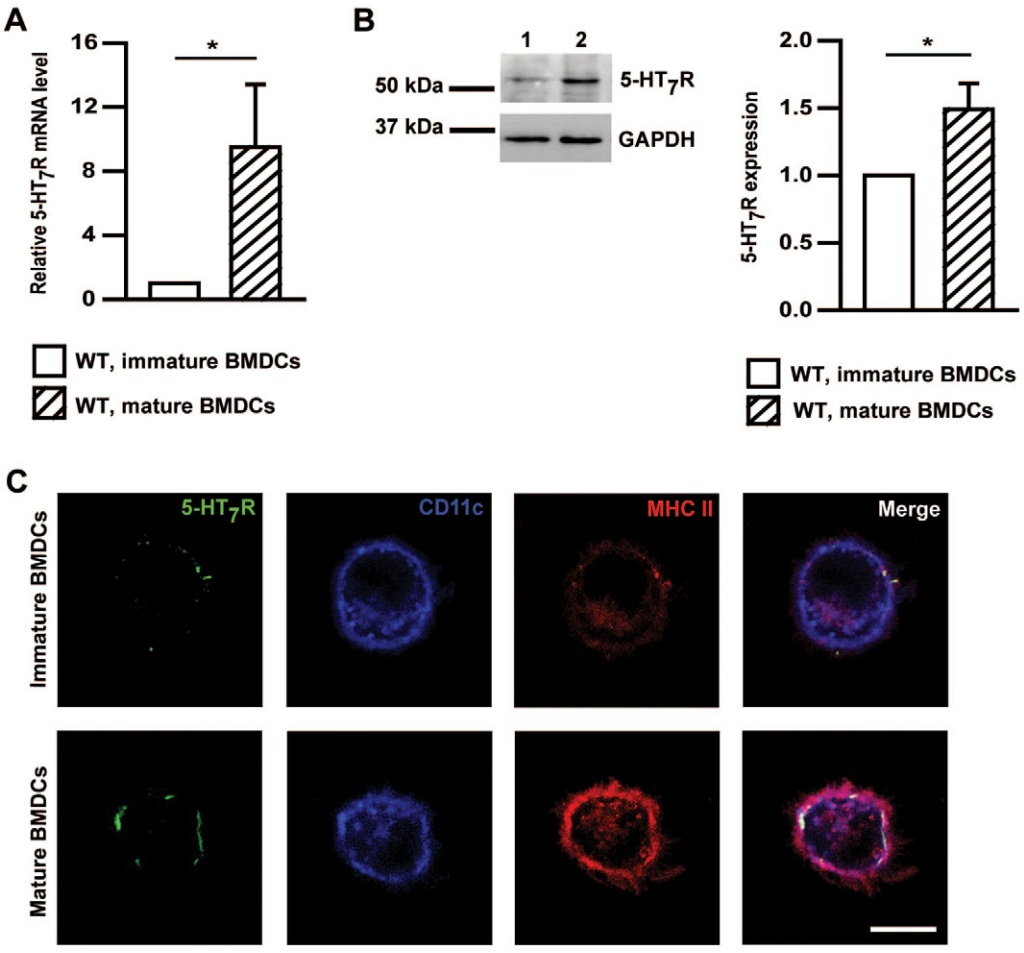

Fig. 1. LPS-induced maturation of BMDCs leads to an increased expression of 5-HT$_7$R. At 8 div, WT BMDCs were treated with H_2O or 1 µg/ml LPS for 24 h (for western blot analysis and immunocytochemistry analysis) or 48 h (for qRT-PCR). For immunocytochemistry analysis, cells were seeded prior to stimulation as 95×10^3 cells/well on 12-mm coverslips. (A) Relative expression level of mRNA encoding for 5-HT$_7$R in immature and mature BMDCs was determined by qRT-PCR (n=5). (B) 5-HT$_7$R protein level was determined by western blot analysis in membrane lysates of immature and mature BMDCs. Lane 1, immature WT BMDCs; lane 2, mature WT BMDCs. A quantitative analysis of western blot results is shown on the right. Levels were normalized to expression of those GAPDH (n=3). Bars represent mean±s.e.m. *P<0.05. (C) Representative images of maximum intensity projections of specific z-stack subsets showing distribution of 5-HT$_7$R in immature and mature BMDCs. Scale bar: 10 µm.

Journal of Cell Science (2015) 128, 2866-2880 doi:10.1242/jcs.167999

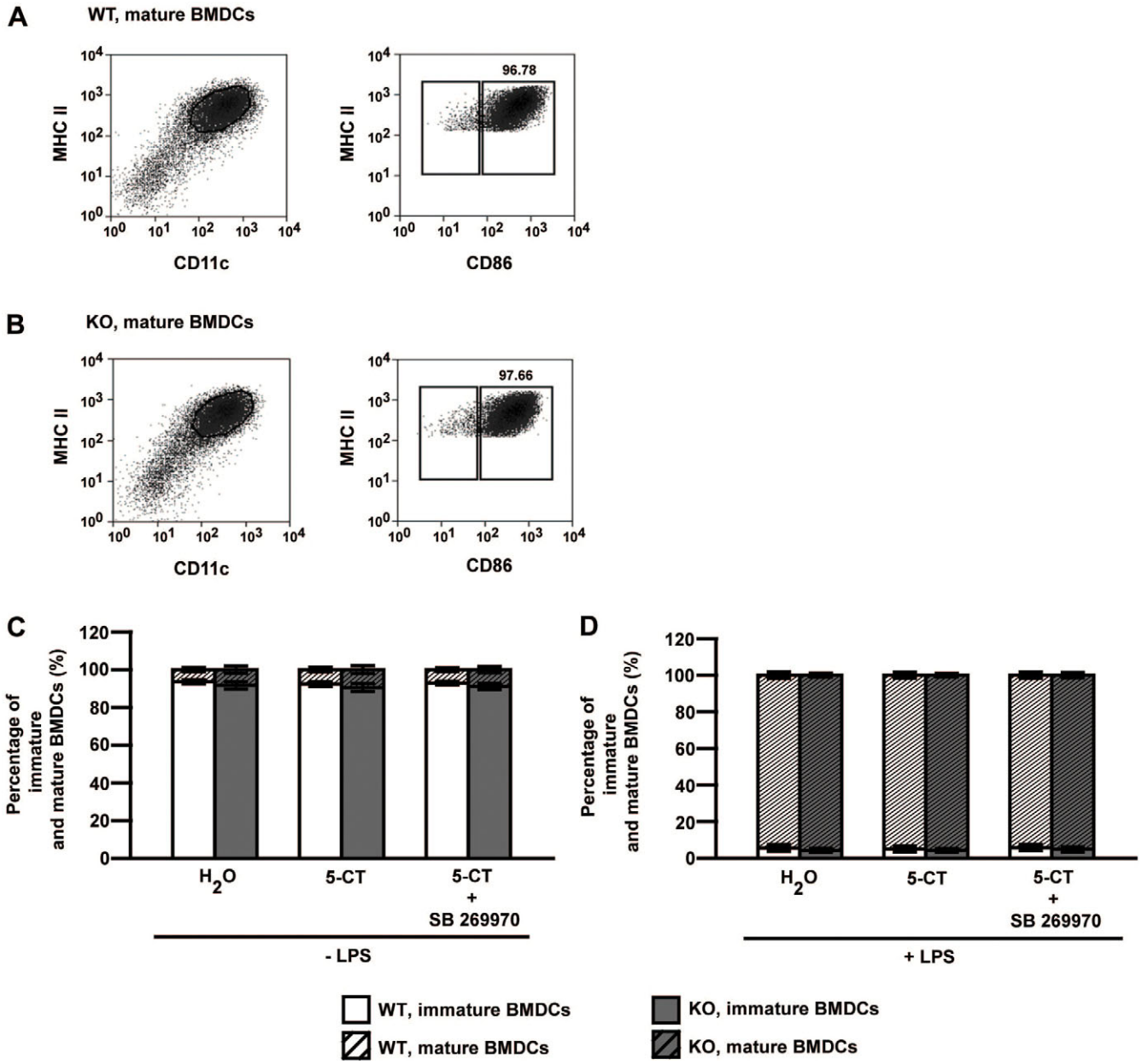

Fig. 2. Differentiation and maturation of BMDCs are not affected by 5-HT$_7$R-mediated signaling. At 8 div, WT and 5-HT$_7$R-KO BMDCs were treated with H_2O or 1 µg/ml LPS for 48 h. Immature and mature BMDCs of both cell lines were additionally treated with 10 µM of the 5-HT$_7$R agonist 5-CT alone or in combination with 10 µM of the 5-HT$_7$R antagonist SB 269970. H_2O was used as a control treatment. Cells were incubated with antibodies against CD11c, MHC II and CD86, followed by flow cytometry analysis. (A,B) Representative images of flow cytometry profiles of mature WT and 5-HT$_7$R-KO BMDCs are shown. The mature population of cells (CD11c^{HIGH}, MHC II^{HIGH} and CD86^{HIGH}) is framed in the right panel on the right side. (C) Quantitative analysis of immature and mature BMDCs in H_2O-treated cultures stimulated with the 5-HT$_7$R agonist 5-CT alone, in combination with 5-HT$_7$R antagonist SB 269970 or with H_2O. (D) Quantitative analysis of the percentage of immature and mature BMDCs in LPS-stimulated cultures treated with the 5-HT$_7$R agonist 5-CT alone, in combination with 5-HT$_7$R antagonist SB 269970 or with H_2O. Bars represent mean±s.e.m. Results from five different cell cultures are shown. P>0.05.

(Fig. 2A,B). Thus, 5-HT$_7$R does not affect differentiation of BMDCs under basal conditions.

Next, we studied the effect of receptor stimulation on BMDC maturation. Immature and mature BMDCs were treated with the 5-HT$_7$R agonist 5-carboxamidotryptamine maleate (5-CT; 10 µM) either alone or in combination with 10 µM of the highly selective 5-HT$_7$R antagonist SB 269970 for 48 h. These concentrations were selected based on previously published data (Amireault and Dube, 2005; Crider et al., 2003; Kvachnina et al., 2005; Saitow et al., 2009). Quantitative analysis of flow cytometry data showed no difference in the number of immature and mature BMDCs after 5-HT$_7$R stimulation (Fig. 2C,D) demonstrating that 5-HT$_7$R-mediated signaling has no influence on the maturation of BMDCs.

Stimulation of 5-HT$_7$R leads to process formation and elongation in mature BMDCs through Cdc42-mediated signaling

We have previously shown that activation of the 5-HT$_7$R–Cdc42 signaling pathway leads to an increased neurite outgrowth and to the formation of dendritic spines in hippocampal neurons (Kvachnina et al., 2005; Ponimaskin et al., 2007). Therefore, we hypothesized that the morphology of dendritic cells, including the events of

Journal of Cell Science (2015) 128, 2866-2880 doi:10.1242/jcs.167999

process formation and elongation, might also be associated with 5-HT$_7$R–Cdc42-mediated signaling. To test this hypothesis, BMDCs isolated from transgenic mice expressing GFP under the control of the β-actin promoter (Berberich et al., 2008; Okabe et al., 1997), were seeded as 95×10^3 cells/well on 12-mm coverslips and stimulated with 1 μg/ml LPS. Cells were incubated with vehicle (H_2O), 10 μM 5-CT alone or 5-CT in combination with 10 μM SB 269970 for 24 h, followed by morphometric analysis. BMDCs were identified by incubation of GFP-expressing cells with antibodies against the specific dendritic cells markers CD11c and CD86 typically expressed by mature dendritic cells (Fig. 3A). The impact of Cdc42 activation on dendritic cell morphology was investigated by treatment of GFP-expressing mature BMDCs with 50 μM of the selective Cdc42 inhibitor ZCL 278 (Friesland et al., 2013) alone or in combination with 5-CT for 24 h.

Morphometric analysis of long-term experiments (24 h) revealed a significant increase in the length of processes in mature BMDCs treated with the receptor agonist in comparison with H_2O-treated control cells (Fig. 3A,B), whereas no significant changes in the number of processes were observed (Fig. 3C). This effect was receptor specific, because it was completely blocked by the treatment with receptor antagonist SB 269970. Interestingly, the inhibition of Cdc42 resulted in a significant reduction in both the length and number of processes, as compared to the vehicle-treated cells (Fig. 3A–C), suggesting the importance of basal Cdc42 activity for BMDC morphology. This effect could not be rescued by receptor stimulation with agonist, further emphasizing that Cdc42-mediated signaling is downstream of 5-HT$_7$R.

Long-term experiments were extended by short-term analysis, where stimulation of cells occurred for 30 min. Similar to results obtained after prolonged treatment, short-term stimulation with 5-CT also led to an increased length of processes, although the effect was less pronounced (supplementary material Fig. S1). Consistent with the results of long-term stimulation experiments, the pharmacological inhibition of Cdc42 alone or along with 5-HT$_7$R stimulation by 5-CT also induced a significant decrease in process length (supplementary material Fig. S1).

The impact of Cdc42 in process formation was further confirmed by the observation that the expression level of Cdc42 was significantly increased in both mature WT and 5-HT$_7$R-deficient BMDCs in comparison to immature cells (Fig. 3D,E). It is noteworthy that 5-HT$_7$R deficiency does not lead to an altered expression of Cdc42 in mature BMDCs, because we obtained a comparable level of Cdc42 in WT and 5-HT$_7$R-deficient BMDCs (supplementary material Fig. S1D). Taken together, these results demonstrate a crucial role of 5-HT$_7$R–Cdc42-mediated signaling in regulation of dendritic cell morphology.

5-HT$_7$R–Cdc42-mediated signaling enhances the chemotactic migration of mature BMDCs in Transwell migration assays

The capacity of dendritic cells to initiate immune responses is dependent on their specific chemotactic migration allowing dendritic cells to reach lymph nodes and to interact with naïve T cells. To analyze the ability of 5-HT$_7$R to induce chemotactic migration of dendritic cells *in vitro*, we subjected BMDCs isolated from WT or 5-HT$_7$R-deficient mice to Transwell migration assays. Cells were transferred on the porous membrane in the upper compartment of Transwell migration chambers, accompanied with 5-HT$_7$R agonist treatment either in the upper or lower compartment chamber. The number of cells migrated to the lower compartment was determined after 24 h. These experiments demonstrate that mature BMDCs do not possess a chemotactic response to 5-HT$_7$R activation with 5-CT (Fig. 4A). In addition, the CXCL12-induced BMDC migration was not influenced by the 5-HT$_7$R stimulation with 5-CT (supplementary material Fig. S2A). CXCL12 is a ligand of CXCR4 receptor known to induce strong chemotactic migration of immature dendritic cells.

To analyze whether 5-HT$_7$R stimulation can modulate the chemotactic behavior of mature dendritic cells, we transferred mature WT and 5-HT$_7$R-deficient BMDCs to the upper compartment of the Transwell chamber and added 0.1 μg/ml C-C motif chemokine 19 (CCL19) to the lower chamber compartment. CCL19 is a ligand of the chemokine receptor CCR7 (Ricart et al., 2011; Sallusto et al., 1999; Vecchi et al., 1999; Yanagihara et al., 1998) and a strong activator of mature dendritic cell migration (Sozzani et al., 1998). The concentration of 0.1 μg/ml CCL19 was selected in accordance with previous data indicating a maximal chemotactic response at this concentration (Ricart et al., 2011; Yoshida et al., 1998). In parallel, 10 μM of the 5-HT$_7$R agonist 5-CT, either alone or in combination with 10 μM of the 5-HT$_7$R antagonist SB 269970, was added to the upper Transwell compartment. The role of Cdc42 activity was elucidated by the pre-treatment of cells with 50 μM ZCL 278, a selective Cdc42 inhibitor, added either alone or in combination with 5-CT. The number of cells migrated to the lower compartment was determined in long-term (analysis after 24 h) and in short-term (analysis after 5 h) experiments.

Quantitative analysis of long-term experiments revealed that CCL19 induces a strong chemotactic movement of mature WT BMDCs with a chemotactic index of 7.9±0.2 (mean±s.e.m., n=3), whereas the chemotactic index of mature 5-HT$_7$R-knockout (KO) BMDCs was reduced to 5±0.5 (Fig. 4B). Stimulation of 5-HT$_7$R with 5-CT results in a further increase of the chemotactic index to 10.4±0.4 in WT BMDCs, whereas no significant chemotactic index changes appeared in 5-HT$_7$R-deficient BMDCs upon 5-CT treatment (chemotactic index of 5.6±0.5; Fig. 4B). Application of the 5-HT$_7$R-specific antagonist SB 269970 in combination with receptor stimulation leads to a strong and significant decrease of CCL19-induced chemotaxis in mature WT BMDCs (chemotactic index of 6.5±0.1 versus 10.4±0.4), demonstrating that the 5-CT-induced increase in chemotactic index was mediated by 5-HT$_7$R. This was further confirmed by the observation that combined application of 5-CT and SB 269970 had no significant influence on the chemotactic movement of 5-HT$_7$R-deficient BMDCs (chemotactic index of 4.7±0.9).

Treatment of mature WT BMDCs with Cdc42 inhibitor caused no significant changes in chemotactic index (9±0.5) in comparison to WT cells treated only with CCL19 (Fig. 4B). In contrast, the increase in chemotactic motility obtained upon 5-HT$_7$R stimulation with 5-CT was completely abolished upon simultaneous Cdc42 inhibition with ZCL 278 (chemotactic index of 10.4±0.4 versus 5.5±0.2), suggesting that 5-HT$_7$R-mediated Cdc42 activation is important for the chemotactic dendritic cell motility. Treatment of 5-HT$_7$R-deficient BMDCs with ZCL 278 either alone or in combination with 5-CT did not demonstrate any significant changes of the chemotactic index, when compared with 5-HT$_7$R-deficient control cells (chemotactic index of 4.8±1.4 and 3.3±1.3 versus 5±0.5; Fig. 4B).

Similar to results obtained in long-term stimulation experiments, quantitative analysis of short-term experiments revealed that CCL19 induced a strong chemotactic movement of mature WT BMDCs with a chemotactic index of 12.2±1.7, whereas the chemotactic index of mature 5-HT$_7$R-KO BMDCs was reduced to 6.9±0.3 (supplementary material Fig. S3). In addition, the treatment of mature WT and 5-HT$_7$R-deficient BMDCs with Cdc42 inhibitor

Journal of Cell Science (2015) 128, 2866-2880 doi:10.1242/jcs.167999

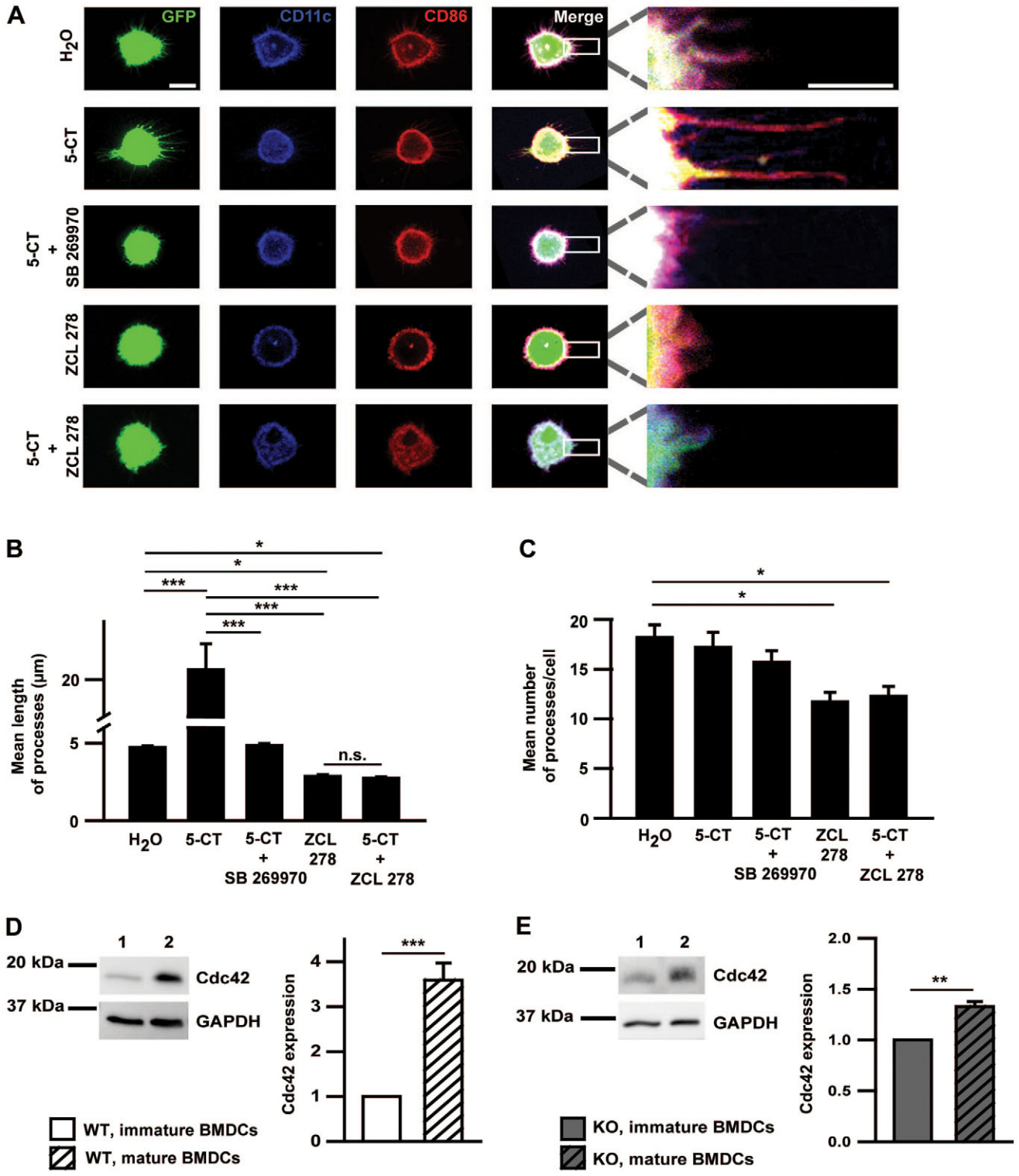

Fig. 3. 5-HT$_7$R-mediated signaling is involved in process elongation in mature BMDCs. (A) At 8 div, GFP-transgenic BMDCs were seeded as 95×10^3 cells/well on 12-mm coverslips and treated with 1 µg/ml LPS for 24 h to stimulate maturation of cells. Representative images are maximum intensity projections of *z*-stacks showing GFP-transgenic mature BMDCs after treatment with 10 µM of the 5-HT$_7$R agonist 5-CT, 10 µM of the 5-HT$_7$R antagonist SB 269970 and 50 µM of the Cdc42 inhibitor ZCL 278 as indicated, or with H_2O alone, for 24 h. BMDCs were stained with antibodies against CD11c and CD86, following live-cell imaging. Scale bar: 10 µm. Magnifications of single processes marked with white boxes are shown on the right side. Scale bar: 5 µm. Quantification of mean length of processes (B) and mean number of processes (C) from mature GFP-transgenic BMDCs treated with the 5-CT, SB 269970 and ZCL 278 as indicated, or with H_2O alone. (D,E) Cdc42 protein expression level in whole-cell lysates from immature and mature WT (D) and 5-HT$_7$R-deficient (E) BMDCs was determined using western blot analysis. Lane 1, immature BMDCs; lane 2, mature BMDCs. Results from three different cell cultures are shown. A quantitative analysis of western blot results are shown on the right. Expression levels were normalized to GAPDH. Bars represent mean±s.e.m., H_2O (*n*=65); 5-CT (*n*=55); 5-CT+SB 269970 (*n*=34); ZCL 278 (*n*=28); 5-CT plus ZCL 278 (*n*=39), where *n* is the number of analyzed cells. Results from three different cell cultures are shown. **P*<0.05, ****P*<0.001.

Journal of Cell Science (2015) 128, 2866-2880 doi:10.1242/jcs.167999

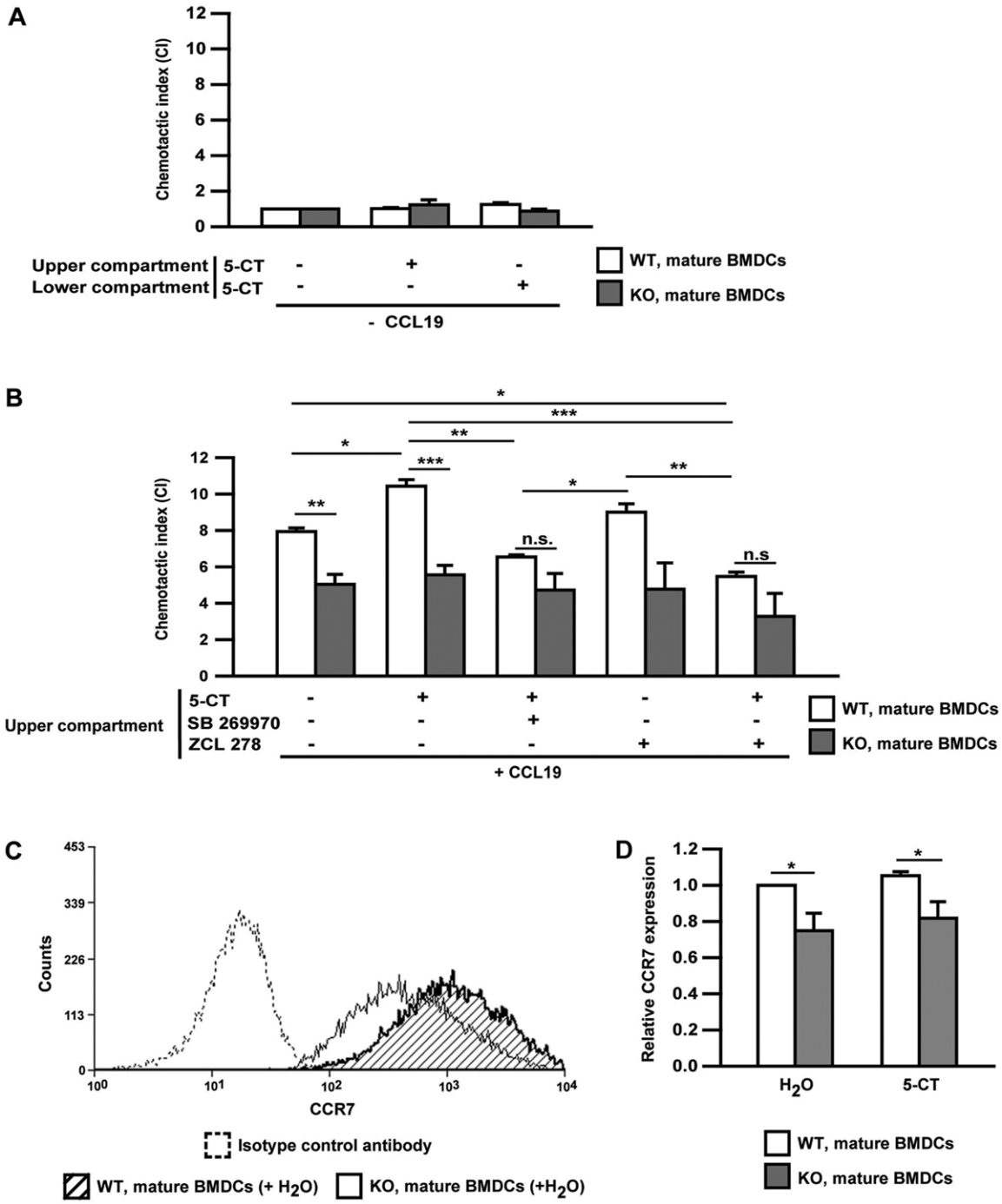

Fig. 4. 5-HT$_7$R signaling enhances chemotactic migration of mature BMDCs in long-term Transwell assays, where expression of the chemokine receptor CCR7 is dependent on 5-HT$_7$R basal activity. At 8 div, WT and 5-HT$_7$R-KO BMDCs were treated with 1 µg/ml LPS for 24 h to stimulated cell maturation. At 9 div, mature WT and 5-HT$_7$R-KO BMDCs were seeded in the upper compartments of Transwell chambers. Flow cytometry analysis of cells collected in lower compartment was performed to obtain the number of migrated BMDCs. (A) Chemotactic index of mature WT and 5-HT$_7$R-KO BMDCs after treatment with H_2O or 10 µM of the 5-HT$_7$R agonist 5-CT in the upper or lower Transwell compartments for 24 h. (B) Chemotactic index of mature WT and 5-HT$_7$R-KO BMDCs after adding 0.1 µg/ml CCL19 to the lower compartment for induction of migration and treatment with H_2O, 50 µM of the Cdc42 inhibitor ZCL 278 alone, 10 µM 5-CT alone or 5-CT in combination with either 10 µM SB 269970 or 50 µM ZCL 278 in the upper Transwell compartment for 24 h. (C) Representative histogram of CCR7 expression profile of WT and 5-HT$_7$R-KO BMDCs provided by flow cytometry analysis. (D) Quantitative analysis of CCR7 expression in mature WT and 5-HT$_7$R-KO BMDCs treated with H_2O or 10 µM 5-CT for 24 h. Values were normalized to the expression of CCR7 in H_2O-treated mature WT BMDCs. Bars represent mean±s.e.m. from at least three independent experiments. *P<0.05, **P<0.01, ***P<0.001.

ZCL 278 resulted in pronounced inhibition of chemotactic motility (chemotactic index of WT 1.5±0.4 and 1.6±0.7; chemotactic index of KO 0.8±0.1 and 1.4±0.3). It is noteworthy that, in short-term experiments, 5-CT treatment was not sufficient to increase the chemotactic index of WT BMDCs, as it was obtained after prolonged stimulation (chemotactic index 12.05±2.1), suggesting that the nature of 5-HT$_7$R-mediated increase of chemotactic movement of BMDCs is complicated.

Journal of Cell Science

Journal of Cell Science (2015) 128, 2866-2880 doi:10.1242/jcs.167999

To analyze the molecular mechanisms underlying 5-HT_7R-mediated facilitation of chemotactic dendritic cell motility in more details, we compared the expression profile of CCR7 in mature WT and 5-HT_7R-deficient BMDCs treated with 10 µM 5-CT or H_2O for 24 h. Analysis of flow cytometry data revealed a significantly reduced expression of the chemokine receptor in 5-HT_7R-deficient BMDCs when compared with WT cells under basal conditions (Fig. 4C,D). In contrast, the CCR7 expression profile was not affected upon 5-HT_7R activation with 5-CT (supplementary material Fig. S4A,B), indicating that basal 5-HT_7R activation is sufficient for proper CCR7 expression.

In addition to CCR7, mature dendritic cells also express CXCR4 receptor and thus could respond to CXCL12. However, it has been shown that CCL19 is a ~100-fold more potent chemoattractant for mature dendritic cells than CXCL12. Furthermore, mature dendritic cells show a strong decrease in the chemotactic response to CXCR4 ligands, demonstrating that the CXCL12–CXCR4 axis is much less important for migration of mature dendritic cells, as compared to CCR7 (Humrich et al., 2006; Ricart et al., 2011). Based on these findings, together with our observation that CXCL12-mediated migration of immature dendritic cells was not modulated by the 5-HT_7R (supplementary material Fig. S2B), we did not further study the role of 5-HT_7R in modulating CXCR4-mediated chemotactic responses in mature dendritic cells.

Taken together, we conclude that 5-HT_7R per se does not possess chemotactic properties. However, the presence of 5-HT_7R plays an important role for CCL19-induced chemotaxis of mature BMDCs, most probably by regulating the expression of CCR7. Our data also demonstrate that 5-HT_7R-induced Cdc42 activation is involved in the control of chemotactic motility of mature BMDCs.

5-HT_7R-mediated signaling enhances directionality of migrating BMDCs in a 3D collagen gel

Although a Transwell assay is commonly used for analysis of chemotaxis (Honig et al., 2003; Ledgerwood et al., 2008; Yopp et al., 2005), it does not allow the measurement of migration velocities and directionality (Tayalia et al., 2011). In contrast, the collagen-based 3D system for analysis of chemotactic cell migration is widely accepted as a system allowing detailed analysis of migration and is a better system to recapitulate the physiological cell environment (Lämmermann et al., 2008, 2009). Therefore, we extended our analysis to 3D collagen gels, which mimic a complex fibrillar scaffold obtained in intact tissues. In this experiment, collagen gels containing mature WT or 5-HT_7R-KO BMDCs were cast in custom-made migration chambers and overlaid with medium containing 0.1 µg/ml CCL19. The role of 5-HT_7R in chemotactic migration was validated by treatment of cells either with 10 µM 5-CT or 5-CT together with 10 µM SB 269970. Cell migration was analyzed by time-laps microscopy and single-cell tracking for 5 h (Fig. 5A,B). In accordance with results obtained in the Transwell system, both cell types (WT and 5-HT_7R-KO) migrated along the chemokine gradient. However, the directionality (i.e. the ratio between the euclidean distance and accumulated distance) of WT BMDCs was significantly higher compared to that of 5-HT_7R-deficient cells (Fig. 5A–C; supplementary material Movies 1 and 2), suggesting the impact of basal receptor activity for defined migration directionality. This was further confirmed by the observation that treatment of WT BMDCs with receptor antagonist resulted in a decrease of directionality to the values obtained for 5-HT_7R-deficient BMDCs (Fig. 5C). Activation of 5-HT_7R by 5-CT led to a significantly increased directionality in WT BMDCs when compared with control cells (0.60±0.02 versus 0.53±0.02, mean±s.e.m., n=4, Fig. 5C). Neither application of 5-HT_7R agonist nor antagonist influenced 5-HT_7R-KO BMDC directionality when compared with control H_2O-treated 5-HT_7R-KO cells (Fig. 5C).

Additionally, we investigated the role of 5-HT_7R activity in regulating migration velocity of BMDCs. As shown in Fig. 5D, the migration velocity of cells was significantly reduced in both antagonist-treated WT BMDCs and untreated 5-HT_7R-deficient BMDCs, when compared with control WT BMDCs (1.68±0.05 µm/min and 1.75±0.05 µm/min versus 1.91±0.05 µm/min). It is noteworthy, that no significant changes in mean velocity were obtained between differently treated 5-HT_7R-deficient BMDCs (Fig. 5D). Taken together, these results suggest that 5-HT_7R plays an important role in the regulation of chemotactic motility of BMDCs in 3D collagen environment by modulating directionality and migration velocity.

5-HT_7R-mediated signaling increases velocity of migratory active intestinal dendritic cells in colon

To extend our observations to the *in vivo* situation, we analyzed the migration behavior of dendritic cells in colon explants from CD11c–EYFP transgenic mice. In this transgenic mouse line, the enhanced yellow fluorescent protein (EYFP) is placed under the control of the CD11c promoter, allowing an unaltered live-cell imaging without any further labeling procedures. Moreover, in our previous study we have demonstrated that a large proportion of the EYFP-expressing cells possess markers described to be characteristic for dendritic cells (Lindquist et al., 2004; Voedisch et al., 2012). Dendritic cell migration was analyzed by two-photon time-lapse microscopy in longitudinally opened colon sections with the lamina propria placed upside and the muscle layer downside after treatment with 1 µg/ml LPS. The impact of 5-HT_7R was investigated by treatment of preparations with 10 µM of the 5-HT_7R antagonist SB 269970 or H_2O, for 1 h. To ensure that only dendritic cells within the colon epithelium were captured for the analysis, additional second harmonic generation (SHG) signals of collagen fibers were collected. The collagen fibers closely underlie the colon epithelium and therefore represent suitable markers for in-tissue orientation. For motility analysis, only EYFP-positive cells colocalizing with collagen fibers were evaluated (Fig. 6A). Trajectories analysis revealed that after pharmacological blockade of 5-HT_7R with antagonist, dendritic cells show a reduced and diffuse migration path, when compared with straight and long-distance moving control cells (Fig. 6B). In accordance with these observations, the mean migration distance of dendritic cells in preparations treated with 5-HT_7R antagonist was significantly decreased in comparison to control dendritic cells [Fig. 6C; 112±5.9 µm for LPS plus H_2O (N=7; n=343 and 61.4±3.4 µm for LPS SB 269970 (N=6; n=231); N is the number of performed experiments and n the number of analyzed cells]. These results demonstrate that 5-HT_7R-mediated signaling can modulate the motility of dendritic cells *in vivo* by regulating their migration velocity.

DISCUSSION

In the present study, we analyzed the impact of 5-HT_7R-mediated signaling in the regulation of dendritic cell functions with a particular focus on dendritic cell morphology and motility. The ability of dendritic cells to prime naïve T cells within the draining lymph nodes and to initiate immune responses is dependent on their chemotactic migration. Leukocyte migration is known to be mainly driven by cell shape changes mediated by rearrangements of the cytoskeletal actin network (Fenteany and Glogauer, 2004; Lämmermann et al., 2008). In this context, members of the Rho family of small GTPases, whose most prominent feature is the

Journal of Cell Science

Journal of Cell Science (2015) 128, 2866-2880 doi:10.1242/jcs.167999

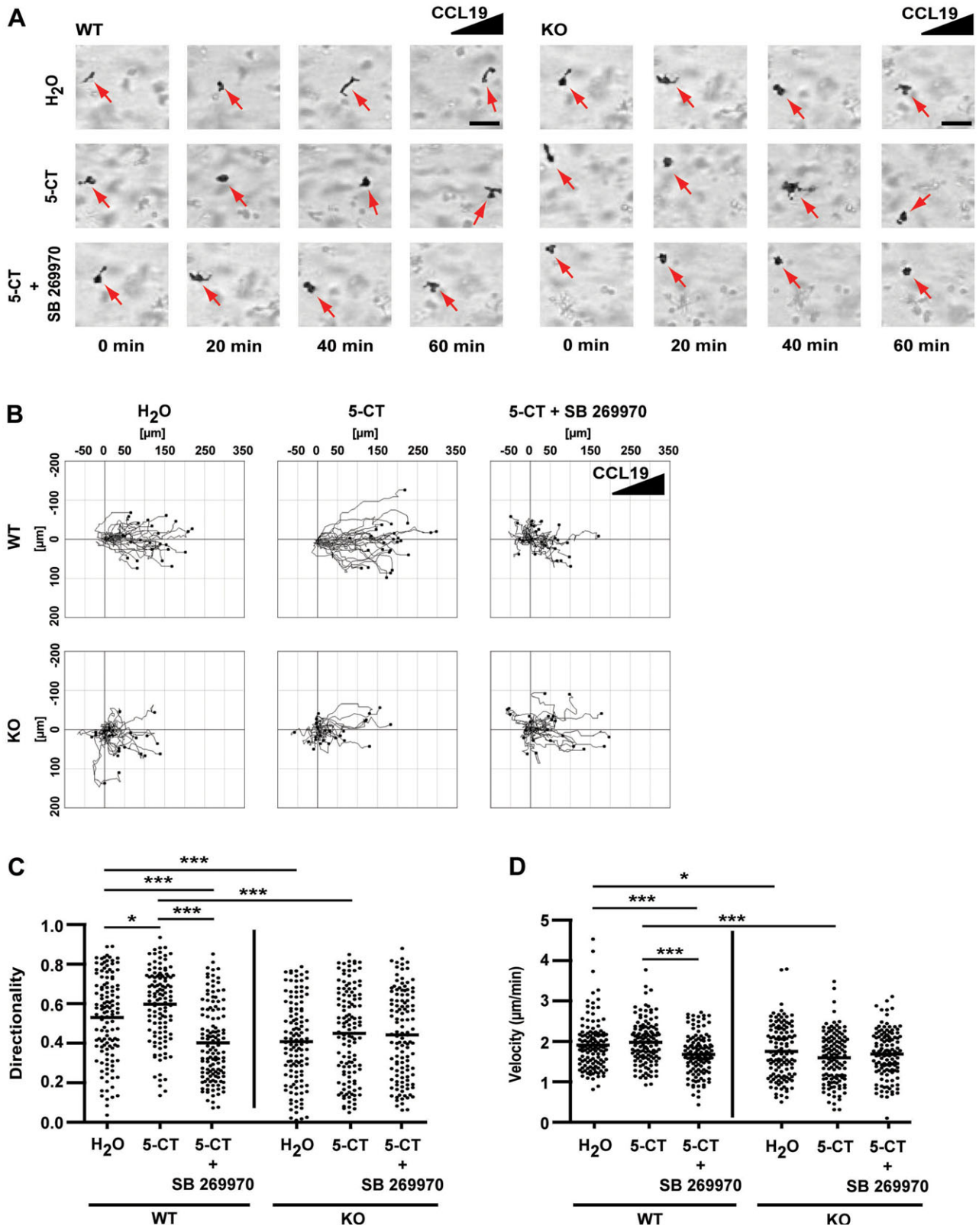

Fig. 5. 5-HT$_7$R-signaling enhances migration directionality and velocity of mature BMDCs isolated from WT, but not from 5-HT$_7$R-KO, mice in 3D collagen gel. At 8 div, WT and 5-HT$_7$R-KO BMDCs were treated with 0.1 µg/ml LPS for 24 h to stimulate cell maturation. (A) Representative images illustrate directionality and velocity of cell migration towards a CCL19 gradient in a 3D collagen matrix for mature WT (left) and 5-HT$_7$R-KO (right) BMDCs over the period of the first 60 min. Cells were stimulated with H_2O, 10 µM 5-CT alone or 5-CT in combination with 10 µM SB 269970. Scale bars: 50 µm. Arrows indicate cell positions. (B) Trajectory plots of migrating mature WT (upper panels) and 5-HT$_7$R-KO (lower panels) BMDCs towards a CCL19 gradient are shown. For every condition, 25 tracked single cells are displayed. Quantitative analysis of mean directionality (C) and velocity (D) of mature WT and 5-HT$_7$R-KO BMDCs in a 3D collagen matrix. Results from four different cell cultures are shown; 25 cells per condition were tracked. *P<0.05, ***P<0.001.

Journal of Cell Science

Journal of Cell Science (2015) 128, 2866-2880 doi:10.1242/jcs.167999

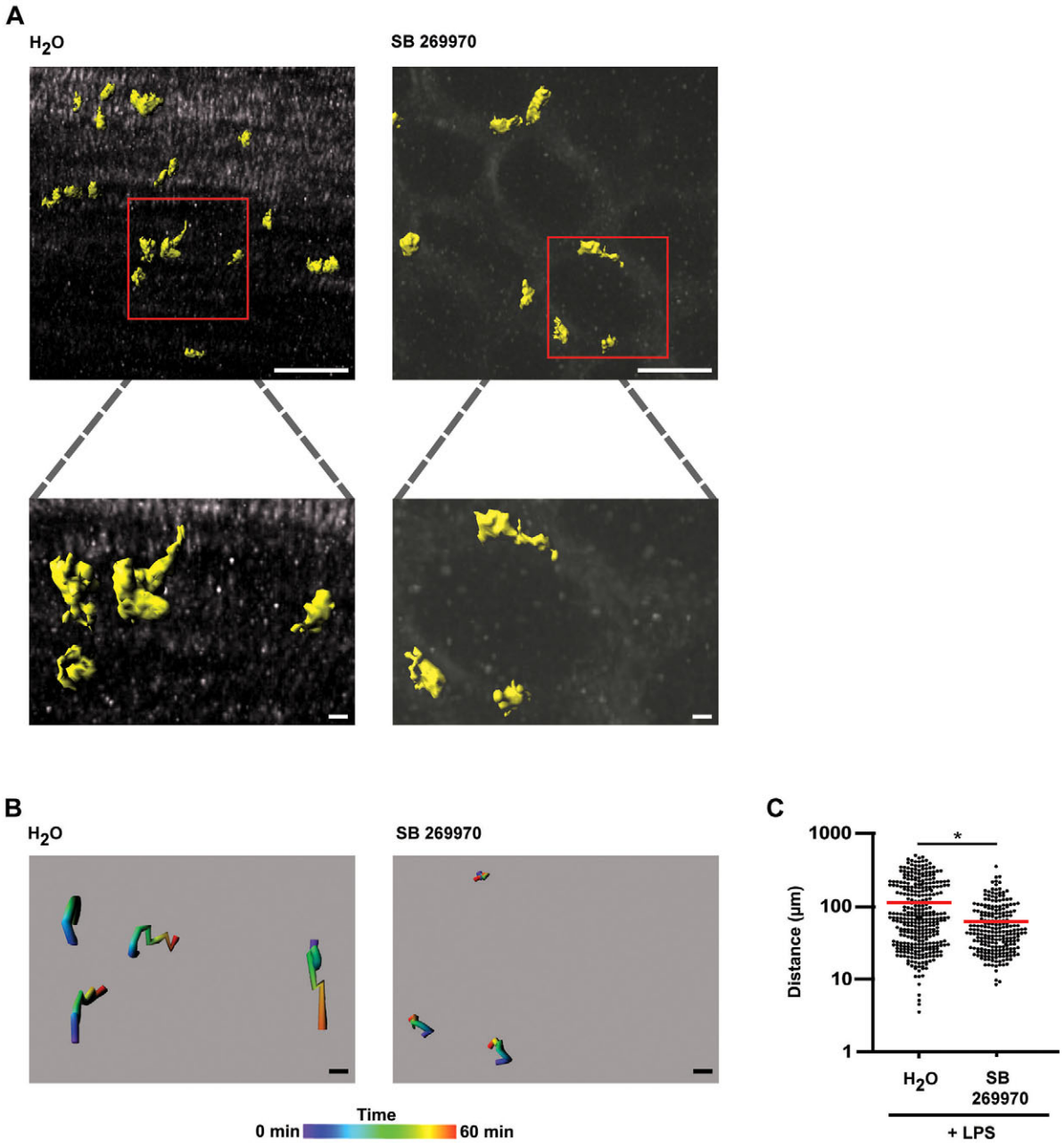

Fig. 6. Inhibition of 5-HT$_7$R signaling decreases the velocity of migratory-active dendritic cells in mouse colon. Colons of CD11c–EYFP transgenic mice were opened longitudinally and 5- to 10-cm-long segments were subjected to experiments. Segments were treated with 0.1 µg/ml LPS for induction of dendritic cell maturation and additionally with either 10 µM of the 5-HT$_7$R antagonist SB 269970 or H_2O. Migration of CD11c–EYFP dendritic cells was imaged for 1 h with a two-photon microscope. (A) A representative image of LPS and H_2O (left) or LPS- and SB 269970-treated (right) colon segments is shown. A 3D stack projection at a single time point of the analysis is shown from the top. Scale bars: 40 µm. A higher magnification of the framed CD11c–EYFP dendritic cells in LPS and H_2O (left) or LPS- and SB 269970-treated (right) colon segments is shown below. Scale bars: 5 µm. CD11c–EYFP-expressing dendritic cells are shown in yellow. The SHG signal of collagen fibers of the colon is shown in gray. (B) Trajectories of CD11c–EYFP-expressing dendritic cells after treatment with LPS and H_2O (left) or LPS and SB 269970 (right). Color-coded scale bar: purple, 0 min; red, 60 min. Scale bars: 5 µm. (C) Quantitative analysis of migrated distance of CD11c–EYFP-expressing colon-derived dendritic cells within 1 h. LPS plus H_2O (n=7; n=343), LPS plus SB 269970 (N=6; n=231), where N is the number of performed experiments and n the number of analyzed cells. *P<0.05.

regulation of the actin cytoskeleton (Hall, 1994; Machesky and Hall, 1997; Norman et al., 1994) represent key players that are crucially involved in the regulation of dendritic cell migratory properties (Benvenuti et al., 2004; Harada et al., 2012; Lammermann et al., 2009; Ocana-Morgner et al., 2011). Our previous data have indicated that, in neurons, actin cytoskeleton rearrangements can be regulated by 5-HT$_7$R through the G_{12} protein-mediated activation of the small GTPase Cdc42 (Kobe et al., 2012; Kvachnina et al., 2005; Nobes and Hall, 1995a,b). We have also demonstrated a high basal activity of 5-HT$_7$R towards Cdc42 signaling in neuronal cells (Kvachnina et al., 2005), suggesting that both basal activity and agonist-mediated stimulation of the 5-HT$_7$R–Cdc42 signaling pathway might contribute to morphological rearrangements of cells. Referring to dendritic cell morphology, Cdc42 has previously been shown to modulate cell shape changes by inducing alterations in the length and number of

Journal of Cell Science (2015) 128, 2866-2880 doi:10.1242/jcs.167999

membrane protrusions, and it is required for the induction and maintenance of the typical stellate cytoskeletal architecture of mature dendritic cells (Jaksits et al., 2004; Nikolic et al., 2011; Swetman et al., 2002). Furthermore, it has been shown that Cdc42 deficiency induces a more rounded morphology in cultured cells (Chen et al., 2000; Wu et al., 2007). Similar results have also been obtained under *in vivo* conditions (Luckashenak et al., 2013), where authors observed a reduced number of protrusions and more rounded morphology in Cdc42-deficient Langerhans cells. Although the significance of small GTPases for morphogenesis of dendritic cells is well established, the upstream signaling components regulating Cdc42-mediated pathways in dendritic cells, as well as its role in the regulation of dendritic cell motility have not been fully characterized.

In the present study, we found that expression of 5-HT$_7$R at both the mRNA and the protein level was upregulated in mature dendritic cells, suggesting an elevated functional mode and the enhancement of receptor-mediated downstream signaling that might be involved in the regulation of dendritic cell functions. Our data also demonstrate that 5-HT$_7$R-mediated signaling modulates morphology as well as the migratory capacity of dendritic cells and that Cdc42 is crucially involved in these processes. Accordingly, we obtained increased protein expression of Cdc42 in mature BMDCs. Reorganization of actin filaments results not only in morphological changes, but is also highly involved in cell motility and migration events that are essential for proper responses to tissue damage as well as infection and for the control of immune surveillance (Kaibuchi et al., 1999; Raftopoulou and Hall, 2004; Ridley, 2001). Cdc42 has also been previously revealed as an important regulator of cell polarity by stabilizing spatial and temporal asymmetries, thereby enabling a clear distinction between cell front and rear to navigate the straight movement of cells (Cau and Hall, 2005; Etienne-Manneville, 2004; Lauffenburger and Horwitz, 1996; Szczur et al., 2006). Furthermore, we have previously shown that Cdc42 deficiency affects the spatial and temporal coordination of protrusions, thereby entailing the development of multiple competing leading edges in the presence of chemoattractant CCL19, which leads to decreased directionality of cells. This finding suggests that Cdc42 is not only involved in formation and/or elongation of protrusions, but also important for the reorganization of these protrusions in leading edges thus enabling proper migration towards chemoattractant (Lammermann et al., 2009). Results of the current study identify 5-HT$_7$R as an important upstream regulator of Cdc42-mediated signaling involved in dendritic cell migration. Receptor stimulation induces an enhanced chemotactic capacity, which was accompanied and therefore attributed to an increased directionality and velocity of dendritic cells. Beside the involvement in the regulation of dendritic cell motility *in vitro*, 5-HT$_7$R-mediated signaling was here additionally demonstrated to be essentially involved in proper dendritic cell migration in colon.

Results of *in vitro* Transwell analysis suggest that 5-HT$_7$R-mediated signaling might modulate dendritic cell migration not only through activation of Cdc42, but also by induction of the other small GTPases. In our previous works, we have shown that RhoA can be activated by the 5-HT$_7$R, although to a lesser extent than Cdc42 (Kvachnina et al., 2005; Kobe et al., 2012). In contrast to Cdc42, which propels cell movement by promoting cellular extension and spreading, RhoA mediates detachment and cell rounding through regulation of actin filament rearrangements (Graness et al., 2006; Hall, 1994, 1998; Sepp and Auld, 2003; Swetman et al., 2002). In dendritic cells, constitutively active mutants of RhoA have been shown to induce cell rounding, unpolarized cell morphology, decreased migration velocity and reduced chemotaxis (Shurin et al., 2005). Thus, the mechanism regulating dendritic cell motility through 5-HT$_7$R might involve a cross-talk between Cdc42 and RhoA (Kvachnina et al., 2005; Li et al., 2002). In this context, a reduced chemotactic capacity of dendritic cells obtained under 5-HT$_7$R stimulation with Cdc42 inhibition in comparison to effect obtained in BMDCs treated only with Cdc42 inhibitor might be attributed to 5-HT$_7$R-mediated activation of RhoA, which results in reduced chemotaxis.

Our data also revealed that 5-HT$_7$R deficiency impairs the expression of the chemokine receptor CCR7 on mature BMDCs. This suggests that beside its role in the regulation of dendritic cell motility through induction of cytoskeletal rearrangements, 5-HT$_7$R-mediated signaling might also affect motility of dendritic cells through regulation of CCR7 expression (Förster et al., 1999; Jang et al., 2006). In accordance with this hypothesis, a previous study reported a reduced ability of maturing Cdc42-deficient dendritic cells to upregulate CCR7 expression (Luckashenak et al., 2013). Furthermore, it has been demonstrated that 5-HT$_7$R-mediated signaling regulates the activation of NF-κB in colon-derived dendritic cells (Kim et al., 2013). By contrast, inhibition of NF-κB has been shown to significantly reduce the induction of CCR7 expression in monocyte-derived dendritic cells (van de Laar et al., 2010). These findings indicate that 5-HT$_7$R–Cdc42-mediated signaling might regulate dendritic cell motility through induction of chemokine receptor CCR7 expression by activation of the NF-κB signaling pathway. Furthermore, 5-HT$_7$R–Cdc42-mediated signaling has been reported to mediate activation of the transcription factor serum response factor (SRF) (Kvachnina et al., 2005). Downregulated expression of SRF target genes paralleled by impaired CCR7 signaling has previously been shown in lesion macrophages of uremic mice (Ponda et al., 2010). In addition, a decreased expression of other SRF-driven genes involved in dendritic cell motility, for example MMP-9 (Yen et al., 2010), could be involved in decreased 3D migration of 5-HT$_7$R-deficient BMDCs. Thus, it would be interesting to analyze in future studies whether the expression of corresponding genes are changed in 5-HT$_7$R-deficient dendritic cells.

Our finding that 5-HT$_7$R can modulate the migratory properties of mature dendritic cells suppose that impaired 5-HT$_7$R-mediated signaling in dendritic cells might be involved in the pathogenesis of inflammatory diseases, which are often accompanied by reduced dendritic cell motility (Angeli and Randolph, 2006; Eriksson and Singh, 2008; Hermida et al., 2014). In our recent work, we have demonstrated that 5-HT$_7$R-mediated signaling is crucially involved in the progression of chemically induced acute and chronic colitis in mice (Guseva et al., 2014). In particular, we observed that pharmacological inhibition as well as genetic ablation of 5-HT$_7$R result in increased severity of intestinal inflammation in both acute and chronic colitis. In addition, in mice with dextran sulfate sodium (DSS)-induced colitis as well as in mucosa biopsies from patients with Crohn's disease, we obtained a highly increased expression level of 5-HT$_7$R and this increase was attributed to 5-HT$_7$R expression on CD11c/CD86 double-positive immune cells. The results of the present study might provide the molecular mechanism explaining the increased inflammatory response obtained upon inhibition of 5-HT$_7$R. Inactivation of 5-HT$_7$R-mediated signaling will result in impaired cytoskeletal rearrangements and reduced expression of CCR7 on dendritic cells leading to decreased directionality and migration velocity of cells as well as to their decelerated motility. Thus, dendritic-cell-mediated activation of specific T cell subsets to induce immune responses against foreign antigens as well as to mediate tolerance to self-antigens will be

Journal of Cell Science (2015) 128, 2866-2880 doi:10.1242/jcs.167999

delayed. Furthermore, impaired 5-HT$_7$R-mediated signaling increases the production of pro-inflammatory cytokines (Guseva et al., 2014). These combined events might exacerbate the severity of inflammatory bowel diseases such as Crohn's disease.

In conclusion, results of the current study reveal that serotonin can modulate motility of dendritic cells by regulating cell morphology, velocity and directionality of migration as well as expression level of the chemokine receptor CCR7 through 5-HT$_7$R–Cdc42-mediated signaling. Our findings represent a new serotonin-mediated mechanism in the regulation of immune cell polarization and pathfinding of dendritic cells and indicate the 5-HT$_7$R could be a new target for the therapy of inflammatory diseases.

MATERIALS AND METHODS

Mice

Mice were bred at the central animal facility of Hannover Medical School (Hannover, NI, Germany) or at Charles River Laboratories (Sulzfeld, BW, Germany). The following mice strains were used: C57BL/6J (wild type, WT), C57BL/6J-Htr7^{tm1Sut} (5-HT$_7$R knockout, 5-HT$_7$R-deficient, 5-HT$_7$R-KO) (Hedlund et al., 2003), C57BL/6-Tg(ACTbEGFP) (designated here as GFP-transgenic mice; these mice constitutively express EGFP in all cells under the control of the β-actin promoter) and CD11c-EYFP transgenic mice (these mice express EYFP under the control of the CD11c promoter) (Berberich et al., 2008; Lindquist et al., 2004; Okabe et al., 1997; Voedisch et al., 2012). This study was conducted in accordance with German law for animal protection and with the European Communities Council Directive 86/609/EEC for the protection of animals used for experimental purposes. All experiments were approved by the Local Institutional Animal Care and Research Advisory committee and permitted by the local government (number 33.14-42502-04-12/0753).

Generation of dendritic cells *in vitro*

Bone marrow-derived dendritic cells (BMDCs) were generated from a flushed bone marrow suspension as previously described (Czeloth et al., 2005). In brief, 5×10^6 bone marrow cells from tibia and femur of WT, 5-HT$_7$R-KO and GFP-transgenic mice were cultured in 10 ml dendritic cell medium containing RPMI 1640 (Invitrogen, Dun Laoghaire, Ireland) with 10% FCS (Invitrogen, Dun Laoghaire, Ireland), 0.0035% β-mercaptoethanol (Roth, Karlsruhe, BW, Germany), 1% L-glutamine (Invitrogen, Dun Laoghaire, Ireland) and 1% penicillin-streptomycin (Invitrogen, Dun Laoghaire, Ireland) supplemented with 100–200 ng/ml granulocyte-macrophage colony-stimulating factor (GM-CSF) produced by a NIH-3T3 cell line infected with Psi2-pM5DGM#6 (Ohl et al., 2004). After 3 days *in vitro* (3 div), another 10 ml cell medium supplemented with GM-CSF was added to the cells. At 6 div, half of the culture supernatant was collected, centrifuged at 1200 ***g*** for 10 min at room temperature and the cell pellet was resuspended in 10 ml fresh medium with GM-CSF. The cell suspension was added back to the original plate and cells were cultured. At 8 div, non-adherent cells were collected and centrifuged at 1200 ***g*** for 10 min at room temperature. Cell pellet was resuspended in dendritic cell medium and cells were counted using a hemocytometer. Cells were seeded on petri dishes (TPP, Trasadingen, Switzerland) at 5×10^6 cells/dish in 10 ml dendritic cell medium. To generate mature BMDCs, 1 µg/ml lipopolysaccharide (LPS) (Sigma-Aldrich, Buchs SG, Switzerland) was added to the cell suspensions. To get immature BMDCs, H_2O was added instead. Further treatments of cells for analysis of cell morphology, cell surface marker expression profiles and cell migration behavior were as described in the following sections. At 9 or 10 div, mature and immature WT BMDCs were harvested, respectively.

Flow cytometry

Flow cytometry was performed according to standard procedures. BMDCs were blocked with 5% rat serum (AbD serotec, Hercules, CA) in 3% FCS (Invitrogen, Dun Laoghaire, Ireland) in PBS (140 mM NaCl, 6 mM Na_2HPO_4, 3 mM KCl, 2 mM KH_2PO_4; Roth, Karlsruhe, BW, Germany) for 15 min at 4°C and surface markers were stained for 15 min at 4°C with anti-CD11c (1:200, anti-mouse CD11c, APC conjugated, eBioscience, Vienna, Austria), anti-MHC II (1:200, anti-mouse I-Ab antibody, FITC conjugated, Biolegend, Fell, RP, Germany), anti-CD86 (1:200, anti-mouse CD86, phycoerythrin-conjugated, Biolegend, Fell, RP, Germany) antibodies and DAPI (1:10,000, Sigma-Aldrich, Buchs SG, Switzerland). For CCR7 expression analysis, BMDCs were preliminarily stained with anti-CCR7 [1:40, anti-mouse CD197 (CCR7), phycoerythrin-conjugated, eBioscience, Vienna, Austria] antibody or the isotype-specific control antibody anti-IgG2a (1:40, anti-mouse IgG2a, κ Isotype Ctrl, phycoerythrin-conjugated, Biolegend, Fell, RP, Germany) for 20 min at 37°C. Flow cytometry was performed on LSRII and FACSAria II (both BD Biosciences, Franklin Lakes, NJ). Data were analyzed with Summit 5.1 software (Beckman Coulter Inc., Krefeld, NM, Germany).

To analyze the physiological function of 5-HT$_7$R on the development of BMDCs, LPS-stimulated or H_2O-treated BMDCs were additionally stimulated with 10 µM of the 5-HT$_7$R agonist 5-carboxamidotryptamine maleate (5-CT) (Tocris, Bristol, UK) alone or in combination with 10 µM of the 5-HT$_7$R antagonist SB 269970 hydrochloride (SB 269970) (Tocris, Bristol, UK) at 8 div. To analyze 5-HT$_7$R functions in the regulation of CCR7 expression on mature BMDCs, LPS-stimulated cells were additionally treated with 10 µM of the 5-HT$_7$R agonist 5-CT or H_2O for 24 h. The application of SB 269970 was performed 30 min before 5-CT treatment. H_2O was used as a control. Cells were incubated at 37°C with 5% CO_2. At 10 div, WT and 5-HT$_7$R-KO mature and immature BMDCs were harvested, blocked and incubated with antibodies against MHC II, CD11c and CD86 followed by DAPI solution. Thereafter, cell suspensions were sorted and analyzed for the amount of immature (CD11c^{HIGH}, MHC II^{LOW} and CD86^{LOW}) and mature (CD11c^{HIGH}, MHC II^{HIGH} and CD86^{HIGH}) BMDCs by using the FACSAria IIU or the XDP (both BD Biosciences, Franklin Lakes, NJ) with 405 nm, 488 nm and 640 nm excitation lasers, fitted with a 100 µm nozzle. Data were collected and the total amount of BMDCs as well as the maturation state of each condition was analyzed using Summit 5.1 software (Beckman Coulter Inc., Krefeld, NM, Germany).

Morphological analysis of GFP-transgenic BMDCs

To estimate the role of 5-HT$_7$R activation on dendritic cells morphology, at 8 div, BMDCs were seeded as 95×10^3 cells/well on 12-mm coverslips and treated with 1 µg/ml LPS to stimulate cell maturation. In addition, BMDCs were treated with 10 µM 5-CT alone or in combination with 10 µM SB 269970. To estimate the role of Cdc42 signaling on dendritic cell morphology, LPS-treated cells were incubated with 50 µM of the selective Cdc42 inhibitor ZCL 278 (Tocris, Bristol, UK) alone or in combination with 10 µM 5-CT. Application of SB 269970 and ZCL 278 occurred 30 min before 5-CT administration. In both cases, H_2O was applied for control measurements. Cells were incubated at 37°C with 5% CO_2 for 24 h (long-term analysis). Dendritic cell surface markers were stained with anti-CD11c (1:50, anti-mouse CD11c, APC conjugated, eBioscience, Vienna, Austria) and anti-CD86 (1:50, anti-mouse CD86, phycoerythrin-conjugated, BioLegend, Fell, RP, Germany) antibodies for 30 min at room temperature. For short-term analysis of dendritic cell morphology, stimulation and staining of cells occurred simultaneously for 30 min. Afterwards, dendritic cells were immediately fixed with 4% paraformaldehyde (PFA).

The morphology of BMDCs was analyzed using a Carl Zeiss LSM 780 microscope (Zeiss, Oberkochen, BW, Germany) with a C-Apochromat 40×1.20 NA water-immersion objective. A series of *z*-stacks (with a width of 0.5 µm/stack) were acquired using a 488 nm laser, a 561 nm laser and a 633 nm laser at a pixel count of 1500×1500 with a 43 µm pinhole. The morphology of BMDCs in short-term experiments was analyzed using a Carl Zeiss LSM 780 (Zeiss, Oberkochen, BW, Germany) with a Plan-Apochromat 63×1.40 NA oil-immersion objective. A series of *z*-stacks (with a width of 0.5 µm/stack) were acquired using a 488 nm laser, a 561 nm laser and a 633 nm laser at a pixel count of 800×800 with a 55 µm pinhole. The mean number and length of dendritic cell processes was analyzed manually with Motic images Plus 2.0 (Motic China group Co., Ltd., Xiamen, PO, China). Represented images shown in figures are maximum intensity projections of *z*-stacks.

Journal of Cell Science (2015) 128, 2866-2880 doi:10.1242/jcs.167999

Immunofluorescence analysis of 5-HT$_7$R expression on BMDCs

To analyze cellular distribution of 5-HT$_7$R, on 8 div, BMDCs were seeded as 95×10^3 cells/well on 12-mm coverslips and got additionally stimulated with or without 1 µg/ml LPS to generate immature and mature cells. At 9 div, immature and mature BMDCs were treated with 10% normal goat serum (NGS, Jackson Immuno Research Laboratories, West Grove, PA) in cell medium for 15 min at room temperature to block unspecific binding of antibodies. Afterwards, dendritic cells were incubated with primary antibody against 5-HT$_7$R (1:10, Novus biological, Littleton, CO) for 30 min at room temperature. After washing, cells were treated with secondary antibody (1:400, goat anti-rabbit-IgG conjugated to Alexa Fluor 546, Life Technologies, Carlsbad, CA) for 5-HT$_7$R detection in combination with cell surface marker staining with anti-CD11c [1:50, anti-mouse CD11c, allophycocyanin (APC) conjugated, eBioscience, Vienna, Austria] and anti-MHC II (1:50, anti-mouse I-Ab antibody, FITC conjugated, Biolegend, Fell, RP, Germany) antibodies for 30 min at room temperature. After staining, cells were fixed with 4% PFA (Roth, Karlsruhe, BW, Germany) for 10 min at room temperature. The cellular distribution of 5-HT$_7$R was analyzed using a Carl Zeiss LSM 780 microscope (Zeiss, Oberkochen, BW, Germany) with a Plan-Apochromat 63×1.40 NA oil-immersion objective. A series of *z*-stacks (with a width of 0.4 µm/stack) were acquired from the middle part of the cell using a 488 nm laser, a 561 nm laser and a 633 nm laser at a pixel count of 512×512 and a 50 µm pinhole. Represented images are maximum intensity projections of specific *z*-stack subsets.

Quantitative real-time PCR analysis

To quantify 5-HT$_7$R mRNA level in immature and mature BMDCs, at 10 div, cells were harvested, blocked with rat serum and stained with antibodies against CD11c, MHC II and CD86 as described above. By using FACS analysis, mature (CD11c^{HIGH}, MHCII^{HIGH} and CD86^{HIGH}) and immature dendritic cells (CD11c^{HIGH}, MHCII^{LOW} and CD86^{LOW}) BMDCs were sorted. After sorting, total RNA was isolated and purified by using TRIzol Reagent (Invitrogen, Dun Laoghaire, Ireland), RNeasy mini kit (Qiagen, Hilden, NW, Germany) and an RNase-Free DNase set (Qiagen, Hilden, NW, Germany) according to manufacturer's instructions. RNA was reverse transcribed using the SuperScriptIII First-Strand Synthesis System (Invitrogen, Dun Laoghaire, Ireland). Real-time PCR was performed in triplicates on a StepOnePlus™ real-time PCR system (Applied Biosystems, Darmstadt, HE, Germany) using a TaqMan Universal PCR Master Mix (Applied Biosystems, Darmstadt, HE, Germany). For detection of 5-HT$_7$R mRNA, corresponding Gene Expression Assays containing gene-specific primers were used [5-hydroxytryptamine (serotonin) receptor 7 (Dye:FAM), Mm00434133_m1*, Applied Biosystems, Darmstadt, HE, Germany]. GAPDH was used as a reference gene. Data were collected and analyzed using Step one plus 2.1 software (Applied Biosystems, Darmstadt, HE, Germany) and the analysis was performed by using the comparative CT Method (ΔΔ CT Method) according to the procedure described at: http://www3.appliedbiosystems.com/cms/groups/mcb_support/documents/generaldocuments/cms_042380.pdf.

Preparation of membrane protein extracts and whole-cell lysates

For analysis of 5-HT$_7$R protein expression in BMDCs, on 10 div, mature and immature WT BMDCs were harvested and centrifuged at 1200 ***g*** for 10 min at 4°C. Cells were counted as described above. For the preparation of membrane protein extracts, 10^7 cells were always used. All steps were performed at 4°C. Cell suspensions were centrifuged at 2900 ***g*** for 4 min and cells were homogenized in 150 µl homogenization buffer. Homogenates were centrifuged at 2300 ***g*** for 5 min. Supernatants were collected and centrifuged again at 13,600 ***g*** for 20 min. Cell pellets, containing membrane proteins were resuspended in 50 µM HEPES (Roth, Karlsruhe, BW, Germany) and stored until usage at −80°C.

For analysis of Cdc42 protein expression in BMDCs, on 10 div, mature and immature WT and 5-HT$_7$R-deficient BMDCs were harvested and centrifuged at 1200 ***g*** for 10 min at 4°C. Cells were counted as described above. For the preparation of whole-cell lysates, 10^7 cells were always used. Cell suspensions were centrifuged at 1200 ***g*** for 4 min at 4°C and cell pellets were resuspended in 100 µl MAPK buffer (150 mM NaCl, 50 mM Tris, 0.5% $C_{24}H_{39}NaO_4$, 1% Triton, 0.1% SDS, 1 mM Na_3VO_4, 50 mM NaF,10 mM $Na_2H_2P_2O_7$; Roth, Karlsruhe, BW, Germany) containing 1% Clap and 1% PMSF (both Roth, Karlsruhe, BW, Germany). Cells were incubated with buffer for 15 min on a shaker at 4°C. Next, cells were centrifuged at 14,000 ***g*** for 15 min at 4°C and cell pellets were removed. Cell lysates were stored until usage at −20°C.

Immunoblot analysis

Protein samples were analyzed on 12% SDS-polacrylamide gels. Proteins were transferred on nitrocellulose membranes (GE Healthcare, Buckingham, UK) (24 h, 40 mA, room temperature), which were then blocked [in 5% dried milk powder in TBS-T (0.2 M Tris, 5 M NaCl, 0.1% Tween 20; Roth, Karlsruhe, BW, Germany) or 5% bovine serum albumin (BSA; Roth, Karlsruhe, BW, Germany) in TBS-T, 1 h, room temperature] and probed with rabbit monoclonal antibody directed against 5-HT$_7$R (Abcam, Milton, UK) or mouse antibody directed against Cdc42 (BD Bioscience, Franklin Lakes, NJ). Membranes were developed with peroxidase-conjugated goat anti-rabbit-IgG antibody (Thermo Fisher Scientific Inc., Waltham, MA) or peroxidase-conjugated goat anti-mouse-IgG antibody (Calbiochem, Bad Soden, HE, Germany). Membranes were developed by chemiluminescence staining using 'super signal western femto maximum sensitifity substrate' (Thermo Fisher Scientific Inc., Waltham, MA) according to the manufacturer's instructions. The chemiluminescence was detected on a Fusion SL advanced MP with a 16-bit CCD camera (Peqlab, Erlangen, BY, Germany). Expression levels of 5-HT$_7$R and Cdc42 proteins were normalized to GAPDH expression and evaluated using the ImageQuant TL software (GE Healthcare, Buckingham, UK).

Two-photon microscopy

12-month-old CD11c-EYFP-transgenic mice were killed by cervical dislocation. Colons were isolated, washed with PBS containing 3% FCS (Invitrogen, Dun Laoghaire, Ireland) and opened longitudinally.

Colon sections of 5 to 10 cm length were covered by 3 ml cell medium (DMEM with F-12, Life Technologies, Carlsbad, CA) and kept in place by a slice anchor within an imaging chamber. Sections were treated with 1 µg/ml LPS for dendritic cells activation alone or in combination with 10 µM of the 5-HT$_7$R antagonist SB 269970. Imaging was performed for 1 h at 37°C with a TriMScope two-photon microscope (La Vision BioTec, Bielefeld, NRW, Germany) attached to a Titanium Sapphire MaiTai HP ultrafast laser (Spectra-Physics, Mountain view, CA) using a 20× water immersion objective. Control and SB 269970-treated (10 µM) sections were imaged alternately on the same day. To make sure that only dendritic cells of the colon epithelium were captured for analysis, the second harmonic generation (SHG) signal of collagen fibers was collected. For motility measurements, only cells colocalizing with these collagen fibers and being defined as EYFP-expressing colon dendritic cells were included. SHG signals of collagen fibers and EYFP fluorescence of CD11c–EYFP transgenic cells were excited with 920 nm (10.25% of 2.65 W output power) and detected by 490/50 or 525/50 band pass filters, respectively. To generate four-dimensional time-lapse images of moving CD11c–EYFP cells each 5 min of 1 h *z*-stacks were acquired with a 1 mm z-resolution resulting in image volumes of 500 mm in the *xy*- and 30 to 60 mm in the *z*-direction. Image stacks were combined to volumes using Imaris version 6.5.3 (Bitplane AG, Zürich, Switzerland) and the location of cells was determined using the 'surpass mode spot tracking' function. Cells with a diameter of 10 µm (mature dendritic cells) were marked in their center with a spot-to-track cell movement. To subtract peristaltic movement of the colon containing dendritic cells chosen for analysis, the 'translational drift correction' function was applied on resting single cells, lying within the collagen fibers with SHG signal.

Transwell migration assay

At 9 div, lower chambers of Transwell plates (6.5 mm Transwell, 5.0 µm Pore Polycarbonate Membrane Insert, Corning, NY) were filled with medium containing RPMI 1640 (Invitrogen, Dun Laoghaire, Ireland), 0.0035% β-mercaptoethanol (Roth, Karlsruhe, BW, Germany), 1% L-glutamine (Invitrogen, Dun Laoghaire, Ireland) and 1% penicillin/streptomycin (Invitrogen, Dun Laoghaire, Ireland). The chemokines CCL19 for mature BMDCs and CXCL12 for immature BMDCs

(both Peprotech, Rocky Hill, NJ, diluted in RPMI 1640) were added as 0.1 µg/ml. H_2O was used as control. 1×10^5 mature or immature WT or 5-HT_7R-KO BMDCs were resuspended in 100 µl cell medium were transferred into the upper chamber. To verify the role of Cdc42 signaling on dendritic cell migration behavior, mature BMDCs were treated in the upper chamber with 50 µM ZCL 278 alone or in combination with 10 µM 5-CT. To estimate the role of 5-HT_7R on dendritic cell migration behavior, BMDCs were treated in the upper chamber with 10 µM 5-CT alone or in combination with 10 µM SB 269970 hydrochloride. Application of SB 269970 and ZCL 278 occurred 30 min before 5-CT administration. H_2O was applied as control. For long-term experiments, cells were incubated at 37°C with 5% CO_2 for 24 h. For analysis, cells from lower chambers were collected and cell numbers were evaluated with the LSRII and FACSAria II (BD Biosciences, Franklin Lakes, NJ) and Summit 5.1 software (Beckman Coulter Inc., Krefeld, NM, Germany). For short-term experiments, cells were incubated at 37°C with 5% CO_2 for 5 h. For analysis, cells from lower chambers were collected and cell numbers were evaluated using a hemocytometer. All conditions were performed in duplicates. The chemotactic index was calculated as the ratio between numbers of dendritic cells migrated in the presence and in the absence of stimuli (i.e. chemotatic index=dendritic cells migrated with stimuli/dendritic cells migrated without stimuli).

3D collagen gel migration assay

The 3D collagen gel chemotaxis assay was performed as described previously (Lammermann et al., 2009). Briefly, at 9 div, mature WT and 5-HT_7R-KO BMDCs were washed once with PBS. Cells were resuspended in RPMI medium containing RPMI 1640 (Invitrogen, Dun Laoghaire, Ireland), 0.0035% β-mercaptoethanol (Roth, Karlsruhe, BW, Germany), 1% L-glutamine (Invitrogen, Dun Laoghaire, Ireland) and 1% penicillin-streptomycin (Invitrogen, Dun Laoghaire, Ireland). Cells were added in a 1:2 ratio to a collagen mix containing PureCol (Advanced biomatrix, San Diego, CA) in MEM (Invitrogen, Dun Laoghaire, Ireland) and 0.4% sodium bicarbonate (Sigma-Aldrich, Buchs SG, Switzerland). The end concentration of collagen gels was 1.6 mg/ml and final cell number for one assay was 4×10^5 dendritic cells/ml. 5-HT_7R stimulation and inhibition was performed by adding 10 µM 5-CT alone or in combination with 10 µM SB 269970. For control measurements, H_2O was applied. Collagen–cell mixtures were transferred in a custom-made migration chamber with a thickness of 0.5 to 1 mm. After 30 min, as assembly of the collagen fibers occurred at 37°C, the gels were overlaid with 0.1 µg/ml CCL19 (Peprotech, Rocky Hill, NJ) diluted in RPMI 1640. Low-magnification bright-field movies of 3D collagen chemotaxis assays were recorded for 5 h at 1-min intervals in custom-built climate chambers (5% CO_2, 37°C, humidified) and PAL camera (Prosilica, Vancouver, Canada) triggered by custom-made software (SVS Vistek, Seefeld, BY, Germany). Dendritic cells were tracked over 2 h with ImageJ (National Institutes of Health, Bethesda, MD) and the manual tracking plugin Velocity (µm/min) and directionality (ratio between euclidean distance and accumulated distance, $0\leq$values≤1) parameters were calculated and visualized as plots by analyzing the acquired data with the chemotaxis and migration tool Plugin.

Statistical analysis

Statistical analyses were performed with Sigma Plot 11.0 (Systat software Inc., San Jose, CA) and GraphPad prism 5 (GraphPad software Inc., San Diego, CA) software using one-way and two-way ANOVA with Bonferroni and Fisher post-hoc corrections, respectively. All experiments were performed three times at least. All data shown as bar graphs represent mean±s.e.m. Statistical differences for the mean values are indicated as follows: *P<0.05; **P<0.01; ***P<0.001.

Competing interests

The authors declare no competing or financial interests.

Author contributions

K.H., E.P., D.G., O.P., A.B. and M.S. conceived the study. K.H., D.G., S.S., M.S., A.B., H.S. and O.P. were responsible for experimental design. K.H., D.G., S.S., M.S. and O.P. performed experiments. K.H., S.S., D.G. and E.P. analyzed the data. K.H., D.G., E.P., S.S., A.B. and M.S. provided reagents, materials and/or analysis tools. K.H., D.G. and E.P. wrote the paper.

Funding

These studies were supported by the Deutsche Forschungsgemeinschaft (DFG) [grant number PO732 and REBIRTH project to E.P.].

Supplementary material

Supplementary material available online at
http://jcs.biologists.org/lookup/suppl/doi:10.1242/jcs.167999/-/DC1

References

Ahern, G. P. (2011). 5-HT and the immune system. *Curr. Opin. Pharmacol.* **11**, 29-33.

Albayrak, A., Halici, Z., Cadirci, E., Polat, B., Karakus, E., Bayir, Y., Unal, D., Atasoy, M. and Dogrul, A. (2013). Inflammation and peripheral 5-HT receptors: the role of 5-HT receptors in carrageenan induced inflammation in rats. *Eur. J. Pharmacol.* **715**, 270-279.

Amireault, P. and Dubé, F. (2005). Intracellular cAMP and calcium signaling by serotonin in mouse cumulus-oocyte complexes. *Mol. Pharmacol.* **68**, 1678-1687.

Angeli, V. and Randolph, G. J. (2006). Inflammation, lymphatic function, and dendritic cell migration. *Lymphat. Res. Biol.* **4**, 217-228.

Banchereau, J. and Steinman, R. M. (1998). Dendritic cells and the control of immunity. *Nature* **392**, 245-252.

Banchereau, J., Briere, F., Caux, C., Davoust, J., Lebecque, S., Liu, Y.-J., Pulendran, B. and Palucka, K. (2000). Immunobiology of dendritic cells. *Annu. Rev. Immunol.* **18**, 767-811.

Barnes, N. M. and Sharp, T. (1999). A review of central 5-HT receptors and their function. *Neuropharmacology* **38**, 1083-1152.

Benvenuti, F., Hugues, S., Walmsley, M., Ruf, S., Fetler, L., Popoff, M., Tybulewicz, V. L. J. and Amigorena, S. (2004). Requirement of Rac1 and Rac2 expression by mature dendritic cells for T cell priming. *Science* **305**, 1150-1153.

Berberich, S., Dahne, S., Schippers, A., Peters, T., Muller, W., Kremmer, E., Forster, R. and Pabst, O. (2008). Differential molecular and anatomical basis for B cell migration into the peritoneal cavity and omental milky spots. *J. Immunol.* **180**, 2196-2203.

Cau, J. and Hall, A. (2005). Cdc42 controls the polarity of the actin and microtubule cytoskeletons through two distinct signal transduction pathways. *J. Cell Sci.* **118**, 2579-2587.

Chen, F., Ma, L., Parrini, M. C., Mao, X., Lopez, M., Wu, C., Marks, P. W., Davidson, L., Kwiatkowski, D. J., Kirchhausen, T. et al. (2000). Cdc42 is required for PIP2-induced actin polymerization and early development but not for cell viability. *Curr. Biol.* **10**, 758-765.

Crider, J. Y., Williams, G. W., Drace, C. D., Katoli, P., Senchyna, M. and Sharif, N. A. (2003). Pharmacological characterization of a serotonin receptor (5-HT7) stimulating cAMP production in human corneal epithelial cells. *Invest Ophthalmol. Vis. Sci.* **44**, 4837-4844.

Czeloth, N., Bernhardt, G., Hofmann, F., Genth, H. and Forster, R. (2005). Sphingosine-1-phosphate mediates migration of mature dendritic cells. *J. Immunol.* **175**, 2960-2967.

Dienz, O. and Rincon, M. (2009). The effects of IL-6 on CD4T cell responses. *Clin. Immunol.* **130**, 27-33.

Dürk, T., Panther, E., Müller, T., Sorichter, S., Ferrari, D., Pizzirani, C., Di Virgilio, F., Myrtek, D., Norgauer, J. and Idzko, M. (2005). 5-Hydroxytryptamine modulates cytokine and chemokine production in LPS-primed human monocytes via stimulation of different 5-HTR subtypes. *Int. Immunol.* **17**, 599-606.

Eriksson, A. U. and Singh, R. R. (2008). Cutting edge: migration of langerhans dendritic cells is impaired in autoimmune dermatitis. *J. Immunol.* **181**, 7468-7472.

Etienne-Manneville, S. (2004). Cdc42 - the centre of polarity. *J. Cell Sci.* **117**, 1291-1300.

Fenteany, G. and Glogauer, M. (2004). Cytoskeletal remodeling in leukocyte function. *Curr. Opin. Hematol.* **11**, 15-24.

Figdor, C. G., de Vries, I. J. M., Lesterhuis, W. J. and Melief, C. J. M. (2004). Dendritic cell immunotherapy: mapping the way. *Nat. Med.* **10**, 475-480.

Förster, R., Schubel, A., Breitfeld, D., Kremmer, E., Renner-Müller, I., Wolf, E. and Lipp, M. (1999). CCR7 coordinates the primary immune response by establishing functional microenvironments in secondary lymphoid organs. *Cell* **99**, 23-33.

Friesland, A., Zhao, Y., Chen, Y.-H., Wang, L., Zhou, H. and Lu, Q. (2013). Small molecule targeting Cdc42-intersectin interaction disrupts Golgi organization and suppresses cell motility. *Proc. Natl. Acad. Sci. USA* **110**, 1261-1266.

Graness, A., Giehl, K. and Goppelt-Struebe, M. (2006). Differential involvement of the integrin-linked kinase (ILK) in RhoA-dependent rearrangement of F-actin fibers and induction of connective tissue growth factor (CTGF). *Cell Signal* **18**, 433-440.

Hall, A. (1994). Small GTP-binding proteins and the regulation of the actin cytoskeleton. *Annu. Rev. Cell Biol.* **10**, 31-54.

Hall, A. (1998). Rho GTPases and the actin cytoskeleton. *Science* **279**, 509-514.
Harada, Y., Tanaka, Y., Terasawa, M., Pieczyk, M., Habiro, K., Katakai, T., Hanawa-Suetsugu, K., Kukimoto-Niino, M., Nishizaki, T., Shirouzu, M. et al. (2012). DOCK8 is a Cdc42 activator critical for interstitial dendritic cell migration during immune responses. *Blood* **119**, 4451-4461.
Hedlund, P. B. (2009). The 5-HT7 receptor and disorders of the nervous system: an overview. *Psychopharmacology* **206**, 345-354.
Hedlund, P. B., Danielson, P. E., Thomas, E. A., Slanina, K., Carson, M. J. and Sutcliffe, J. G. (2003). No hypothermic response to serotonin in 5-HT7 receptor knockout mice. *Proc. Natl. Acad. Sci. USA* **100**, 1375-1380.
Hermida, M. D. R., Doria, P. G., Taguchi, A. M. P., Mengel, J. O. and dos-Santos, W. L. C. (2014). Leishmania amazonensis infection impairs dendritic cell migration from the inflammatory site to the draining lymph node. *BMC Infect. Dis.* **14**, 450.
Honig, S. M., Fu, S., Mao, X., Yopp, A., Gunn, M. D., Randolph, G. J. and Bromberg, J. S. (2003). FTY720 stimulates multidrug transporter- and cysteinyl leukotriene-dependent T cell chemotaxis to lymph nodes. *J. Clin. Invest.* **111**, 627-637.
Hubo, M., Trinschek, B., Kryczanowsky, F., Tuettenberg, A., Steinbrink, K. and Jonuleit, H. (2013). Costimulatory molecules on immunogenic versus tolerogenic human dendritic cells. *Front. Immunol.* **4**, 82.
Humrich, J. Y., Humrich, J. H., Averbeck, M., Thumann, P., Termeer, C., Kampgen, E., Schuler, G. and Jenne, L. (2006). Mature monocyte-derived dendritic cells respond more strongly to CCL19 than to CXCL12: consequences for directional migration. *Immunology* **117**, 238-247.
Idzko, M., Panther, E., Stratz, C., Muller, T., Bayer, H., Zissel, G., Durk, T., Sorichter, S., Di Virgilio, F., Geissler, M. et al. (2004). The serotoninergic receptors of human dendritic cells: identification and coupling to cytokine release. *J. Immunol.* **172**, 6011-6019.
Jaksits, S., Bauer, W., Kriehuber, E., Zeyda, M., Stulnig, T. M., Stingl, G., Fiebiger, E. and Maurer, D. (2004). Lipid raft-associated GTPase signaling controls morphology and CD8+ T cell stimulatory capacity of human dendritic cells. *J. Immunol.* **173**, 1628-1639.
Jang, M. H., Sougawa, N., Tanaka, T., Hirata, T., Hiroi, T., Tohya, K., Guo, Z., Umemoto, E., Ebisuno, Y., Yang, B.-G. et al. (2006). CCR7 is critically important for migration of dendritic cells in intestinal lamina propria to mesenteric lymph nodes. *J. Immunol.* **176**, 803-810.
Kaibuchi, K., Kuroda, S. and Amano, M. (1999). Regulation of the cytoskeleton and cell adhesion by the Rho family GTPases in mammalian cells. *Annu. Rev. Biochem.* **68**, 459-486.
Kim, J. J., Bridle, B. W., Ghia, J.-E., Wang, H., Syed, S. N., Manocha, M. M., Rengasamy, P., Shajib, M. S., Wan, Y., Hedlund, P. B. et al. (2013). Targeted inhibition of serotonin type 7 (5-HT7) receptor function modulates immune responses and reduces the severity of intestinal inflammation. *J. Immunol.* **190**, 4795-4804.
Kobe, F., Guseva, D., Jensen, T. P., Wirth, A., Renner, U., Hess, D., Muller, M., Medrihan, L., Zhang, W., Zhang, M. et al. (2012). 5-HT7R/G12 signaling regulates neuronal morphology and function in an age-dependent manner. *J. Neurosci.* **32**, 2915-2930.
Kushnir-Sukhov, N. M., Gilfillan, A. M., Coleman, J. W., Brown, J. M., Bruening, S., Toth, M. and Metcalfe, D. D. (2006). 5-hydroxytryptamine induces mast cell adhesion and migration. *J. Immunol.* **177**, 6422-6432.
Kvachnina, E., Liu, G., Dityatev, A., Renner, U., Dumuis, A., Richter, D. W., Dityateva, G., Schachner, M., Voyno-Yasenetskaya, T. A. and Ponimaskin, E. G. (2005). 5-HT7 receptor is coupled to G alpha subunits of heterotrimeric G12-protein to regulate gene transcription and neuronal morphology. *J. Neurosci.* **25**, 7821-7830.
Lämmermann, T., Bader, B. L., Monkley, S. J., Worbs, T., Wedlich-Söldner, R., Hirsch, K., Keller, M., Förster, R., Critchley, D. R., Fässler, R. et al. (2008). Rapid leukocyte migration by integrin-independent flowing and squeezing. *Nature* **453**, 51-55.
Lammermann, T., Renkawitz, J., Wu, X., Hirsch, K., Brakebusch, C. and Sixt, M. (2009). Cdc42-dependent leading edge coordination is essential for interstitial dendritic cell migration. *Blood* **113**, 5703-5710.
Langenkamp, A., Messi, M., Lanzavecchia, A. and Sallusto, F. (2000). Kinetics of dendritic cell activation: impact on priming of TH1, TH2 and nonpolarized T cells. *Nat. Immunol.* **1**, 311-316.
Lauffenburger, D. A. and Horwitz, A. F. (1996). Cell migration: a physically integrated molecular process. *Cell* **84**, 359-369.
Ledgerwood, L. G., Lal, G., Zhang, N., Garin, A., Esses, S. J., Ginhoux, F., Merad, M., Peche, H., Lira, S. A., Ding, Y. et al. (2008). The sphingosine 1-phosphate receptor 1 causes tissue retention by inhibiting the entry of peripheral tissue T lymphocytes into afferent lymphatics. *Nat. Immunol.* **9**, 42-53.
Li, Z., Aizenman, C. D. and Cline, H. T. (2002). Regulation of rho GTPases by crosstalk and neuronal activity in vivo. *Neuron* **33**, 741-750.
Lindquist, R. L., Shakhar, G., Dudziak, D., Wardemann, H., Eisenreich, T., Dustin, M. L. and Nussenzweig, M. C. (2004). Visualizing dendritic cell networks in vivo. *Nat. Immunol.* **5**, 1243-1250.
Luckashenak, N., Wahe, A., Breit, K., Brakebusch, C. and Brocker, T. (2013). Rho-family GTPase Cdc42 controls migration of Langerhans cells in vivo. *J. Immunol.* **190**, 27-35.
Machesky, L. M. and Hall, A. (1997). Role of actin polymerization and adhesion to extracellular matrix in Rac- and Rho-induced cytoskeletal reorganization. *J. Cell Biol.* **138**, 913-926.
Mikulski, Z., Zaslona, Z., Cakarova, L., Hartmann, P., Wilhelm, J., Tecott, L. H., Lohmeyer, J. and Kummer, W. (2010). Serotonin activates murine alveolar macrophages through 5-HT2C receptors. *Am. J. Physiol. Lung Cell. Mol. Physiol.* **299**, L272-L280.
Mössner, R. and Lesch, K.-P. (1998). Role of serotonin in the immune system and in neuroimmune interactions. *Brain Behav. Immun.* **12**, 249-271.
Müller, T., Dürk, T., Blumenthal, B., Grimm, M., Cicko, S., Panther, E., Sorichter, S., Herouy, Y., Di Virgilio, F., Ferrari, D. et al. (2009). 5-hydroxytryptamine modulates migration, cytokine and chemokine release and T-cell priming capacity of dendritic cells in vitro and in vivo. *PLoS ONE* **4**, e6453.
Nikolic, D. S., Lehmann, M., Felts, R., Garcia, E., Blanchet, F. P., Subramaniam, S. and Piguet, V. (2011). HIV-1 activates Cdc42 and induces membrane extensions in immature dendritic cells to facilitate cell-to-cell virus propagation. *Blood* **118**, 4841-4852.
Nobes, C. D. and Hall, A. (1995a). Rho, rac and cdc42 GTPases: regulators of actin structures, cell adhesion and motility. *Biochem. Soc. Trans.* **23**, 456-459.
Nobes, C. D. and Hall, A. (1995b). Rho, rac, and cdc42 GTPases regulate the assembly of multimolecular focal complexes associated with actin stress fibers, lamellipodia, and filopodia. *Cell* **81**, 53-62.
Norman, J. C., Price, L. S., Ridley, A. J., Hall, A. and Koffer, A. (1994). Actin filament organization in activated mast cells is regulated by heterotrimeric and small GTP-binding proteins. *J. Cell Biol.* **126**, 1005-1015.
Ocana-Morgner, C., Reichardt, P., Chopin, M., Braungart, S., Wahren, C., Gunzer, M. and Jessberger, R. (2011). Sphingosine 1-phosphate-induced motility and endocytosis of dendritic cells is regulated by SWAP-70 through RhoA. *J. Immunol.* **186**, 5345-5355.
O'Connell, P. J., Wang, X., Leon-Ponte, M., Griffiths, C., Pingle, S. C. and Ahern, G. P. (2006). A novel form of immune signaling revealed by transmission of the inflammatory mediator serotonin between dendritic cells and T cells. *Blood* **107**, 1010-1017.
Ohl, L., Mohaupt, M., Czeloth, N., Hintzen, G., Kiafard, Z., Zwirner, J., Blankenstein, T., Henning, G. and Förster, R. (2004). CCR7 governs skin dendritic cell migration under inflammatory and steady-state conditions. *Immunity* **21**, 279-288.
Okabe, M., Ikawa, M., Kominami, K., Nakanishi, T. and Nishimune, Y. (1997). 'Green mice' as a source of ubiquitous green cells. *FEBS Lett.* **407**, 313-319.
Pakala, R. and Benedict, C. R. (1998). Effect of serotonin and thromboxane A2 on endothelial cell proliferation: effect of specific receptor antagonists. *J. Lab. Clin. Med.* **131**, 527-537.
Pakala, R., Willerson, J. T. and Benedict, C. R. (1997). Effect of serotonin, thromboxane A2, and specific receptor antagonists on vascular smooth muscle cell proliferation. *Circulation* **96**, 2280-2286.
Ponda, M. P., Barash, I., Feig, J. E., Fisher, E. A. and Skolnik, E. Y. (2010). Moderate kidney disease inhibits atherosclerosis regression. *Atherosclerosis* **210**, 57-62.
Ponimaskin, E., Voyno-Yasenetskaya, T., Richter, D. W., Schachner, M. and Dityatev, A. (2007). Morphogenic signaling in neurons via neurotransmitter receptors and small GTPases. *Mol. Neurobiol.* **35**, 278-287.
Racké, K., Reimann, A., Schwörer, H. and Kilbinger, H. (1996). Regulation of 5-HT release from enterochromaffin cells. *Behav. Brain Res.* **73**, 83-87.
Raftopoulou, M. and Hall, A. (2004). Cell migration: rho GTPases lead the way. *Dev. Biol.* **265**, 23-32.
Randolph, G. J., Angeli, V. and Swartz, M. A. (2005). Dendritic-cell trafficking to lymph nodes through lymphatic vessels. *Nat. Rev. Immunol.* **5**, 617-628.
Ricart, B. G., John, B., Lee, D., Hunter, C. A. and Hammer, D. A. (2011). Dendritic cells distinguish individual chemokine signals through CCR7 and CXCR4. *J. Immunol.* **186**, 53-61.
Ridley, A. J. (2001). Rho GTPases and cell migration. *J. Cell Sci.* **114**, 2713-2722.
Roses, R. E., Xu, S., Xu, M., Koldovsky, U., Koski, G. and Czerniecki, B. J. (2008). Differential production of IL-23 and IL-12 by myeloid-derived dendritic cells in response to TLR agonists. *J. Immunol.* **181**, 5120-5127.
Saitow, F., Murano, M. and Suzuki, H. (2009). Modulatory effects of serotonin on GABAergic synaptic transmission and membrane properties in the deep cerebellar nuclei. *J. Neurophysiol.* **101**, 1361-1374.
Sallusto, F., Palermo, B., Lenig, D., Miettinen, M., Matikainen, S., Julkunen, I., Forster, R., Burgstahler, R., Lipp, M. and Lanzavecchia, A. (1999). Distinct patterns and kinetics of chemokine production regulate dendritic cell function. *Eur. J. Immunol.* **29**, 1617-1625.
Sepp, K. J. and Auld, V. J. (2003). RhoA and Rac1 GTPases mediate the dynamic rearrangement of actin in peripheral glia. *Development* **130**, 1825-1835.
Shurin, G. V., Tourkova, I. L., Chatta, G. S., Schmidt, G., Wei, S., Djeu, J. Y. and Shurin, M. R. (2005). Small rho GTPases regulate antigen presentation in dendritic cells. *J. Immunol.* **174**, 3394-3400.

Sozzani, S., Allavena, P., D'Amico, G., Luini, W., Bianchi, G., Kataura, M., Imai, T., Yoshie, O., Bonecchi, R. and Mantovani, A. (1998). Differential regulation of chemokine receptors during dendritic cell maturation: a model for their trafficking properties. *J. Immunol.* **161**, 1083-1086.

Steinman, R. M. (1991). The dendritic cell system and its role in immunogenicity. *Annu. Rev. Immunol.* **9**, 271-296.

Steinman, R. M. and Witmer, M. D. (1978). Lymphoid dendritic cells are potent stimulators of the primary mixed leukocyte reaction in mice. *Proc. Natl. Acad. Sci. USA* **75**, 5132-5136.

Steinman, R. M., Hawiger, D., Liu, K., Bonifaz, L., Bonnyay, D., Mahnke, K., Iyoda, T., Ravetch, J., Dhodapkar, M., Inaba, K. et al. (2003). Dendritic cell function in vivo during the steady state: a role in peripheral tolerance. *Ann. N. Y. Acad. Sci.* **987**, 15-25.

Swetman, C. A., Leverrier, Y., Garg, R., Gan, C. H. V., Ridley, A. J., Katz, D. R. and Chain, B. M. (2002). Extension, retraction and contraction in the formation of a dendritic cell dendrite: distinct roles for Rho GTPases. *Eur. J. Immunol.* **32**, 2074-2083.

Szczur, K., Xu, H., Atkinson, S., Zheng, Y. and Filippi, M.-D. (2006). Rho GTPase CDC42 regulates directionality and random movement via distinct MAPK pathways in neutrophils. *Blood* **108**, 4205-4213.

Tamura, K., Kanzaki, T., Saito, Y., Otabe, M., Saito, Y. and Morisaki, N. (1997). Serotonin (5-hydroxytryptamine, 5-HT) enhances migration of rat aortic smooth muscle cells through 5-HT2 receptors. *Atherosclerosis* **132**, 139-143.

Tayalia, P., Mazur, E. and Mooney, D. J. (2011). Controlled architectural and chemotactic studies of 3D cell migration. *Biomaterials* **32**, 2634-2641.

van de Laar, L., van den Bosch, A., van der Kooij, S. W., Janssen, H. L. A., Coffer, P. J., van Kooten, C. and Woltman, A. M. (2010). A nonredundant role for canonical NF-kappaB in human myeloid dendritic cell development and function. *J. Immunol.* **185**, 7252-7261.

Vecchi, A., Massimiliano, L., Ramponi, S., Luini, W., Bernasconi, S., Bonecchi, R., Allavena, P., Parmentier, M., Mantovani, A. and Sozzani, S. (1999). Differential responsiveness to constitutive vs. inducible chemokines of immature and mature mouse dendritic cells. *J. Leukoc. Biol.* **66**, 489-494.

Verdijk, P., van Veelen, P. A., de Ru, A. H., Hensbergen, P. J., Mizuno, K., Koerten, H. K., Koning, F., Tensen, C. P. and Mommaas, A. M. (2004). Morphological changes during dendritic cell maturation correlate with cofilin activation and translocation to the cell membrane. *Eur. J. Immunol.* **34**, 156-164.

Voedisch, S., Rochlitzer, S., Veres, T. Z., Spies, E. and Braun, A. (2012). Neuropeptides control the dynamic behavior of airway mucosal dendritic cells. *PLoS ONE* **7**, e45951.

Wu, X., Li, S., Chrostek-Grashoff, A., Czuchra, A., Meyer, H., Yurchenco, P. D. and Brakebusch, C. (2007). Cdc42 is crucial for the establishment of epithelial polarity during early mammalian development. *Dev. Dyn.* **236**, 2767-2778.

Yanagihara, S., Komura, E., Nagafune, J., Watarai, H. and Yamaguchi, Y. (1998). EBI1/CCR7 is a new member of dendritic cell chemokine receptor that is up-regulated upon maturation. *J. Immunol.* **161**, 3096-3102.

Yen, J.-H., Kong, W. and Ganea, D. (2010). IFN-beta inhibits dendritic cell migration through STAT-1-mediated transcriptional suppression of CCR7 and matrix metalloproteinase 9. *J. Immunol.* **184**, 3478-3486.

Yopp, A. C., Ochando, J. C., Mao, M., Ledgerwood, L., Ding, Y. and Bromberg, J. S. (2005). Sphingosine 1-phosphate receptors regulate chemokine-driven transendothelial migration of lymph node but not splenic T cells. *J. Immunol.* **175**, 2913-2924.

Yoshida, R., Nagira, M., Kitaura, M., Imagawa, N., Imai, T. and Yoshie, O. (1998). Secondary lymphoid-tissue chemokine is a functional ligand for the CC chemokine receptor CCR7. *J. Biol. Chem.* **273**, 7118-7122.